Review Article

phys. stat. sol. (a) **137**, 9 (1993)

Subject classification: 72.20; 71.55; 72.40; S8.15

Department of Low Temperature Physics, Faculty of Physics, M. V. Lomonossov Moscow State University[1])

Carrier Transport and Non-Equilibrium Phenomena in Doped PbTe and Related Materials

By

B. A. AKIMOV, A. V. DMITRIEV, D. R. KHOKHLOV, and L. I. RYABOVA

Contents

1. Introduction

2. Stabilization of the Fermi level in doped lead telluride

3. Impurity levels in the modified lead telluride alloys (MLTA) under changes of temperature, alloy composition, pressure, and magnetic field

3.1 Reconstruction of the energy spectrum of the MLTA under variation in alloy composition
3.2 Reconstruction of the energy spectrum of the MLTA under external pressure
3.3 Energy spectrum of the MLTA in high magnetic fields

4. Non-equilibrium states in the MLTA induced by magnetic field and illumination

4.1 Non-equilibrium states in high magnetic field
4.2 Non-equilibrium processes under IR-illumination

5. Theoretical models of the defects forming the long-living states in PbTe-based materials

6. Carrier kinetics in the modified lead telluride alloys in high electric field

6.1 Carrier scattering mechanisms in $Pb_{1-x}Sn_xTe$
6.2 Hot electron phenomena in $Pb_{1-x}Sn_xTe$; theory
6.3 Hot electron phenomena in $Pb_{1-x}Sn_xTe$(In); experiment
6.4 Properties of PbTe(Ga) in high electric field
6.5 Tunneling spectroscopy of doped lead–tin telluride

7. Optical and photoelectric properties of $Pb_{1-x}Sn_xTe$(In) and PbTe(Ga)

7.1 Optical absorption in the group III-doped lead telluride-based alloys
7.2 Photoconductivity spectra of the indium-doped lead telluride-based alloys
7.3 Peculiarities of the photoconductivity spectra of PbTe(Ga)
7.4 Infrared reflection spectra of indium-doped lead–tin tellurides

[1]) Moscow 119899, Russia.

8. Galvanomagnetic and photoelectric phenomena under combined action of external factors

8.1 Electric and magnetic fields
8.2 Strong magnetic field and infrared illumination
8.3 Electric or microwave fields and infrared illumination

9. Photodetector systems based on $Pb_{1-x}Sn_xTe(In)$: applied aspects

10. Concluding remarks

References

1. Introduction

The physics of semiconductors in its development continually includes in the investigation new materials and new physical phenomena they bring with them. Sometimes the materials that attract attention of the scientific community are completely new as for example the artificial crystals, i.e., superlattices, but often they are a modification of well-known ones. For semiconducting materials the most popular and important method of modification of their properties is the introduction of impurities. Investigation of heavily doped semiconductors is a large and interesting problem in the modern physics of semiconductors [1, 2]. In this review article we will discuss electronic properties of the narrow-gap $A^{IV}B^{VI}$ semiconductors PbTe, $Pb_{1-x}Sn_xTe$ and related materials heavily doped with In, Tl, Ga, and some other impurities that lead to the formation of the long-living localized or quasi-localized electron states in the crystal and thus change substantially the electronic properties of the alloys. We will call these materials modified lead telluride alloys (MLTA).

Except for the scientific interest, the investigations of MLTA are stimulated by extensive use of $A^{IV}B^{VI}$ semiconductors and their alloys in the infrared optoelectronics for manufacturing IR-lasers and detectors for the wavelength range extending from 1 to 40 μm [3]. $A^{IV}B^{VI}$ heterostructures and superlattices are also available [4], which makes $Pb_{1-x}Sn_xTe$ and related materials quite competitive in device applications with other popular modern semiconductors [5].

The influence of a high impurity concentration upon the energy spectrum and electronic properties of $Pb_{1-x}Sn_xTe$ is distinctive and quite different from its effect in other semiconductors such as Ge, Si, or InSb [1, 2, 6]. As in MLTA the effect of the Coulomb forces is drastically reduced due to the extremely high value of the static dielectric constant $\varkappa_0 \approx 10^3$ (see Table 1), the binding energy of a shallow impurity state turns out to be below 1 mK (the small value of the carrier effective mass also contributes to this figure). Correspondingly, neither shallow states nor shallow impurity band can be observed in them.

The strong influence impurities have on the electron properties of $Pb_{1-x}Sn_xTe$ and related materials is connected with the deep states that appear as a result of doping. In contrast to shallow states, deep ones consist of wave functions that belong to many bands. So their energy levels are not connected to any particular band edge and they can be situated in a band as well as in the gap [7]. Depending upon the kind of the doping impurity, the physical properties of the centres and of the doped material as well as the observed effects may be very different. Let us mention here a few examples.

Table 1
Parameters of the band energy dispersion law in $Pb_{1-x}Sn_xTe$ [77, 83] (energy in eV, temperature in K)

electron and hole energy dispersion law, $\varepsilon(p)$, measured from the corresponding band edge	$\frac{p_t^2}{2m_t} + \frac{p_l^2}{2m_l} = \varepsilon(p)\left[1 + \frac{\varepsilon(p)}{E_g}\right]$
energy gap width, E_g	$E_g(x, T) = 0.19 - 0.543x + 4.5 \times 10^{-4} T^2/(T + 50)$
carrier effective masses, m_t and m_l	$m_t(x, T)/m_0 = 0.16E_g(x, T)$ $m_l(x, T)/m_0 = 10.5$
energy distance to the second valence band (Σ extremum), measured from the edge of the conduction band	$\Delta_{c,\Sigma} = -0.33$ ($T = 77$ K, $0 \leqq x \leqq 1$)

The highly localized wave functions of neighbouring centres do not overlap significantly, the Coulomb interaction between carriers at different defects is suppressed, so in some cases the level may be very narrow. The level can pin the Fermi energy, and the pinning ensures a high level of spatial uniformity of electrical properties of the semiconductor, which looks somewhat paradoxically for a heavily doped material. The position of the level with respect to the band edges can be tuned by variation of the alloy composition, so it is possible to obtain solid solutions with desired carrier concentration including very low values if the level lies in the gap so that the semiconductor becomes almost intrinsic. In addition, the pinning of the Fermi level makes electronic properties of MLTA stable against the influence of radiation.

The deep levels can affect the carrier transport in MLTA, too. If the levels lie in a band, they may very effectively scatter carriers with energy close to that of the quasi-localized state by means of the so-called resonant scattering mechanism, which leads to the large mobility reduction [8, 9]. The capture of non-equilibrium carriers by the levels [10 to 12] is another important effect.

But maybe the most prominent feature of MLTA brought about by doping is the appearance of the long-term electronic relaxation processes [13]. They can take place when the level lies in a band as well as when it is in the gap. They are connected with the existence of a barrier at the defect which is similar to the autolocalization one that drastically reduces the rate of carrier transitions between the centre and the band. The long-living states influence significantly non-equilibrium processes in MLTA including hot-electron transport, magneto- and photoconductivity, etc. In particular, the long-term character of the relaxation of the non-equilibrium electron distribution is the reason for the very high photosensitivity of MLTA.

There are many other interesting physical phenomena that were observed in MLTA under the influence of light, magnetic field, microwave field, hydrostatic pressure, etc.

In this article we will give a review of the most important and well established experimental data obtained in MLTA and also of the corresponding theoretical calculations. The structure of the article is evident from the table of contents. We will pay considerable attention to the most informative and unambiguous experimental methods. A large part of the review is devoted to the transport phenomena. Bearing in mind the possible applications, we have

included a description of optical and photoelectric properties of MLTA. In the final section a few interesting experiments are also discussed that still have no clear interpretation, and problems for future investigations are formulated.

2. Stabilization of the Fermi Level in Doped Lead Telluride

As a rule, the charge carrier concentration in lead telluride and its solid solutions is rather high. This fact is caused by the existence of native defects of the crystal lattice, i.e. vacancies and interstitials, which are electrically active in these compounds. The crystals grown from the stoichiometric melts are usually of p-type and the hole concentration exceeds 10^{18} cm^{-3}. The annealing of the crystals under different conditions allows to reduce the charge carrier concentration down to 10^{16} cm^{-3}. This value can be considered as a limit for a material that is not specially doped [14].

A great number of elements have been used for the doping of lead telluride. The first group metals Na, Li, Ag demonstrate mostly effective acceptor behaviour. Effective donors are halogens. The doping of PbTe with these elements can increase the charge carrier concentration up to 10^{20} cm^{-3} [9]. Most of the rare earth metals, as well as the elements of the fifth group, also tend to be donors in PbTe [15]. Eu, Sm, Yb, and Tm are the only rare earth elements which in their monotellurides exist in the 2+ valence state (the others are in the 3+ one). These four elements were expected to be neutral impurities in lead telluride. It has been proved for Eu, but Tm has been found to be a donor [16].

The transition metals also act as donors (Cr, Co, Ni, Ti) or as neutral impurities (Mn). It has been established that the increase of Cr content in PbTe led to a rise of the electron concentration up to 1.3×10^{19} cm^{-3}. This concentration remains constant while the Cr content is increased up to the solubility limit [17]. In PbTe(Ti) the maximum value of the electron concentration $n \approx 7 \times 10^{19}$ cm^{-3} is achieved at $N_{\mathrm{Ti}} \approx 0.3$ at%. The further increase of N_{Ti} up to 0.5 at% does not change the value of n [18].

The most interesting and complete data have been obtained for PbTe doped with IIIB group impurities. For In, Ga, and Tl in PbTe the dependence of n, p on the impurity concentration N_{i} appears to saturate within the solubility regions of the corresponding impurities. The saturation level of the free charge carrier concentration is $n \approx 7 \times 10^{18}$ cm^{-3} for PbTe(In) and $p \approx 10^{20}$ cm^{-3} for PbTe(Tl) even if the material is additionally doped with donors (iodine in PbTe(In), superstoichiometric Pb in PbTe(Tl) or acceptors (Na in PbTe(Tl)) if the concentration of the additional impurity is less than N_{In}, N_{Tl}. These results show that in PbTe(In) and PbTe(Tl), as well as in PbTe(Cr) and PbTe(Ti), a chemical stabilization of the Fermi level is observed. In order to explain the properties of Tl- and In-doped lead telluride, Kaidanov and Ravich [9] have proposed a model of the formation of quasi-local impurity levels that pin the Fermi level (FL) in these compounds.

It has been found that the doping of PbTe with In or Cr up to $N_{\mathrm{i}} \approx 0.5$ at% did not reduce significantly the mobilities of charge carriers μ. In the best single crystal samples of PbTe(In) and PbTe(Cr) μ exceeds 10^5 cm^2/Vs [19, 20] at liquid helium temperature. Taking into account that the electron concentration is rather high, especially in PbTe(Cr), where $n = 1.3 \times 10^{19}$ cm^{-3}, one can conclude that the doping does not affect significantly the kinetic properties of the material. It has been established that in high magnetic fields the magnetoresistance of PbTe(In) saturates in agreement with the theory for homogeneous semiconductors [21]. Fine pictures of Shubnikov-de Haas oscillations have also been observed [22, 23] (see Fig. 1). So PbTe(In) and PbTe(Cr) crystals are not similar to the

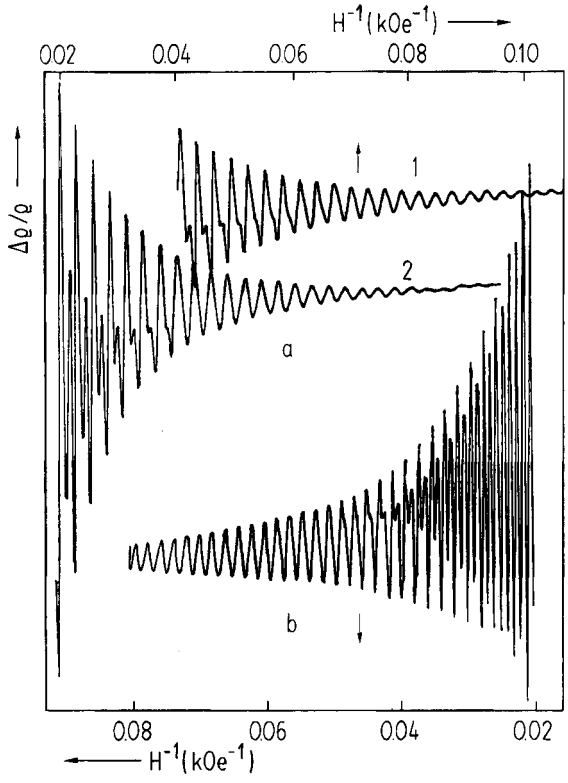

Fig. 1. Recorded $\Delta\varrho/\varrho$ oscillations for a) PbTe(In) (curve 1 represents the enlarged low field region of curve 2) and b) PbTe(Cr); $T = 2.1$ K [54]

ordinary compensated semiconductors where the mobility values appear to be low and the Landau level broadening prevents the observation of oscillatory effects.

For PbTe(Tl) the situation has several peculiarities. For the samples corresponding to the saturation region resonant scattering has been observed (see Section 6). At $N_{Tl} > 5 \times 10^{19}$ cm^{-3} the cross section of hole scattering increases by more than an order of magnitude [8]. The most impressive result is the observation of superconductivity in PbTe(Tl) [24]. The transition temperature depends on the ratio of Tl concentration and the concentration of additional impurities (Li, Na), the hole concentration being constant [25]. The maximum value of the transition temperature achieves 2.2 K, that is a high value for semiconductors.

For Ga-doped PbTe the curve n, $p(N_{Ga})$ has some special features. At least two saturation regions have been observed on this dependence. At low concentrations gallium acts as a donor and converts the type of conductivity of the PbTe crystals from p to n. Just after the conversion the first saturation region is observed. The electron concentration for the samples in this region approaches almost intrinsic values $n < 10^{13}$ cm^{-3} at $T = 77$ K, and the crystals become high-ohmic. The range of N_{Ga} values corresponding to this region seems to depend on the growth methods. PbTe(Ga) single crystals grown by means of a vapour–liquid–solid mechanism stay high-ohmic at GaTe contents in the melt higher than 3 mol% (corresponding to $N_{Ga} \approx 7 \times 10^{19}$ cm^{-3} in the crystal volume) [26]. The crystals grown from the vapour phase appear to be high-ohmic when the GaTe or Ga_2Te_3 content in the source material is equal to 10 mol% [27]. In the crystals obtained with the help of the Czochralski technique the conversion of the conductivity type occurs at $N_{Ga} \approx 10^{19}$ cm^{-3}. At $N_{Ga} \geqq 10^{20}$ cm^{-3} another saturation region is observed. The electron concentration in this region equals $n = 2 \times 10^{18}$ cm^{-3} [28]. According to [29] the solubility limit for Ga in $Pb_{1-x}Ga_xTe$ is achieved at $x = 0.01$, the saturation region exists in the interval (0.15 to 0.75) at% of Ga. In metalloceramic samples one more saturation region has been found at high values of N_{Ga}, n being $\approx 6 \times 10^{19}$ cm^{-3} at $N_{Ga} \approx 5 \times 10^{20}$ cm^{-3} [30]. So the data obtained by different authors are not in good agreement, but for almost all of the PbTe(Ga)

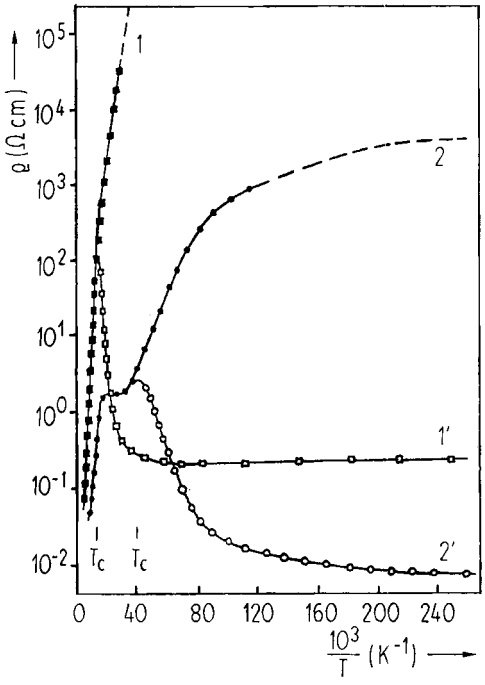

Fig. 2. The temperature dependence of the sample resistivity ϱ measured in the dark (1), (2) and under infrared illumination (1'), (2') in PbTe(Ga) (1), (1') and $Pb_{0.75}Sn_{0.25}Te$(In) (2), (2') [54]

samples $n \ll N_{Ga}$. For the high-ohmic n-type PbTe(Ga) crystals the region corresponding to the impurity activation process has been observed on the temperature dependence of the resistivity ϱ (see Fig. 2) and of the Hall coefficient. With the help of the equation

$$\varrho \sim \exp(E_a/2kT) \tag{2.1}$$

the energy $E_a \approx 140$ meV for the donor impurity level has been determined [31 to 33].

As a conclusion it should be pointed out that doping of lead telluride with different impurities can be considered as a rather complicated process. The dependence of free carrier density on the impurity concentration seems to be non-linear, and in some cases saturation regions within the solubility limit are observed. The existence of these regions cannot be attributed to a definite origin without additional investigation of the material. Besides the FL pinning, the effect of saturation may be caused by self-compensation phenomena. It means that the incorporation of an impurity atom into the crystal lattice under special conditions brings about the formation of a native defect which neutralizes the impurity atom. The self-compensation has been observed in PbTe(Bi) [34], in Zn and Ar ion implanted PbTe films [35, 36], and in PbTe(Cl) [37]. That is why the effect of FL pinning for each substance must be proved by a number of additional experimental facts: high homogeneity of electrical properties throughout the sample volume, the motion of the band edges with respect to the pinned FL under the action of different external factors, such as hydrostatic pressure, magnetic field, or temperature. A detailed experimental investigation has been carried out only for a few impurities in lead telluride. We shall consider the results of this research in the next sections.

3. Impurity Levels in the Modified Lead Telluride Alloys (MLTA) under Changes of Temperature, Alloy Composition, Pressure, and Magnetic Field

The first experiments that proved the existence of the impurity levels and the FL pinning in the conduction band of PbTe were the measurements of the temperature dependence of the Hall coefficient R_H. The results obtained for PbTe(In) [21] and later for PbTe(Cr) [20, 38] qualitatively differ from the data for lead telluride doped with halogens or donor native defects, where R_H stays nearly constant up to rather high temperatures $T > 300$ K. In PbTe(In) and PbTe(Cr) a significant change of the R_H value under temperature variation

has been observed. This effect was explained in terms of the electron concentration variation induced by the pinned FL shift towards the bottom of the conduction band as T rises. The coefficients $\partial E_i/\partial T$ were found to have similar values for PbTe(In) and PbTe(Cr), $-(3 \pm 1) \times 10^{-4}$ eV/K.

The interpretation of the $R_H(T)$ dependence for the p-type material PbTe(Tl) seems to be a more complicated problem because heavy holes from the second valence subband take part in the conductivity process.

3.1 Reconstruction of the energy spectrum of the MLTA under variation in alloy composition

The investigation of the solid solutions based on doped PbTe with pinned FL gives an important information on the origin and properties of the impurity centres. To the present moment a large number of compounds has been studied. Of course, for some of the substances the information is rather brief and insufficient to make any conclusions. But it is interesting to compare all available data with the results for the materials studied in details, for example, with $Pb_{1-x}Sn_xTe$(In). We shall consider the solid solutions $Pb_{1-x}Me_xTe$ in which the atoms are replaced in the metal sublattice. The list of known materials with pinned FL and their main characteristics are represented in Table 2.

It should be mentioned that the conclusion about the FL pinning in solid solutions with variable composition in general needs to be supported by the determination of the n, $p(N_i)$ dependence for every x-value. But this complicated work is done only in a few cases [9]. For the majority of compounds the effect of pinning has been proved using special investigations of the character of the shift of the pinned FL relative to the band edges.

Up to now In and Ga are known to be the only impurities whose incorporation results in the FL pinning not only in PbTe, but in a variety of its solid solutions (see Table 2). Moreover, the shift of FL appears to be nearly linear in x for them. An interesting feature of all In- and Ga-doped solid solutions with both positive and negative values of $\partial E_g/\partial x$ is the negative value of $\partial(E_F - E_c)/\partial x$. In In-doped solid solutions ($Pb_{1-x}Sn_xTe$(In) [39, 40],

Table 2

The main properties of PbTe-based solid solutions with pinned FL. (The values of n, p, and E_F are presented for $T = 4.2$ K, SMSC stands for semimagnetic semiconductor)

PbTe(In)	$n = 6 \times 10^{18}$ cm^{-3}, $E_F - E_c = 70$ meV, $T_c \approx 20$ K
PbTe(Cr)	$n = 1.3 \times 10^{19}$ cm^{-3}, $E_F - E_c = 100$ meV, SMSC
PbTe(Tl)	$p \approx 10^{19}$ cm^{-3}, SC at $T < 3$ K
PbTe(Ga)	$(E_c - E_F) \approx$ (65 to 70) meV, $T_c \approx 80$ K
$Pb_{1-x}Sn_xTe$(In)	$0.22 < x < 0.28$ dielectric state, $T_c \approx 20$ K
$Pb_{1-x}Mn_xTe$	$\partial E_g/\partial x \approx 40$ meV/mol% MnTe, SMSC
$Pb_{1-x}Mn_xTe$(In)	$x > 0.05$ dielectric state, $T_c \approx 20$ K
$Pb_{1-x}Mn_xTe$(Ga)	dielectric state, $T_c \approx 80$ K
$Pb_{1-x}Ge_xTe$(In)	$x > 0.08$ dielectric state, $T_c \approx 20$ K
$Pb_{1-x}Ge_xTe$(Ga)	dielectric state, $T_c \approx 80$ K
$Pb_{1-x}Sn_xTe$(Ga)	pressure induced n-p inversion
$Pb_{1-x-y}Sn_xGe_yTe$(In)	photosensor with variable τ_e

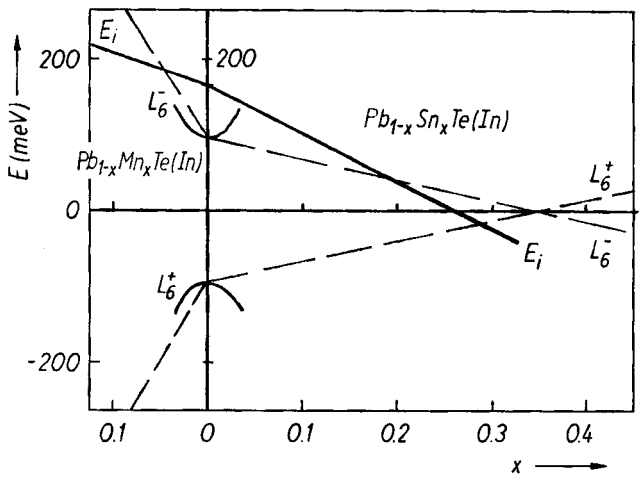

Fig. 3. The diagram representing the reconstruction of the energy spectrum at the variation of the alloy composition x for $Pb_{1-x}Sn_xTe(In)$ and $Pb_{1-x}Mn_xTe(In)$; $T \to 0$

$Pb_{1-x}Mn_xTe(In)$ [41], $Pb_{1-x}Ge_xTe(In)$ [42, 43]) it results in so-called metal–dielectric transitions that occur when FL crosses the edge of one of the allowed bands at some definite x-value. Diagrams illustrating the energy spectrum reconstruction under x-variation are shown in Fig. 3 for $Pb_{1-x}Sn_xTe(In)$ and $Pb_{1-x}Mn_xTe(In)$ alloys. One can see that in the interval $0.22 < x < 0.28$ for $Pb_{1-x}Sn_xTe(In)$ the FL is pinned within the gap [39]. (According to the data obtained in [40] this composition interval is slightly different.) For alloys from this composition range the values of the free carrier concentrations at low temperatures appear to be lower than 10^{10} cm^{-3} at liquid helium temperature. At $x \approx 0.26$ the FL crosses the middle of the gap and the conversion of conductivity from n- to p-type is observed. For $Pb_{1-x}Mn_xTe(In)$ the metal–dielectric transition is observed at $x \approx 0.05$. It should be noted that $Pb_{1-x}Mn_xTe$ solid solutions exist only at $x < 0.20$, and In-doped ones have been investigated only for $x < 0.1$ [29]. The metal–dielectric transition is also observed in $Pb_{1-x}Ge_xTe(In)$ at $x \approx 0.08$ [42, 43]. The In impurity has been found to reduce significantly the temperature of the ferroelectric phase transition in $Pb_{1-x}Ge_xTe$, that is why it is difficult to present a diagram of the energy spectrum reconstruction for this alloy.

3.2 Reconstruction of the energy spectrum of the MLTA under external pressure

One more factor varying the relative position of the band edges and the pinned FL is the hydrostatic pressure P. It has been found out that in $Pb_{1-x}Sn_xTe(In)$ with different x-values the FL slightly shifts relative to the middle of the energy gap under pressure [44], while the band extrema L_6^+ and L_6^- at first move towards each other and, after the gapless state is achieved at $P = P_i$, move apart. The gapless state indicates the point where band inversion takes place. In the direct energy spectrum region L_6^- forms the conduction band, L_6^+ forming the valence one, and vice versa in the inverse spectral region. The diagram of the energy spectrum reconstruction under pressure is represented in Fig. 4 for alloys with different composition. For the $Pb_{1-x}Sn_xTe(In)$ alloys in the dielectric state the successive transitions, dielectric–metal–dielectric have been observed at $P = P_1$, P_2, respectively.

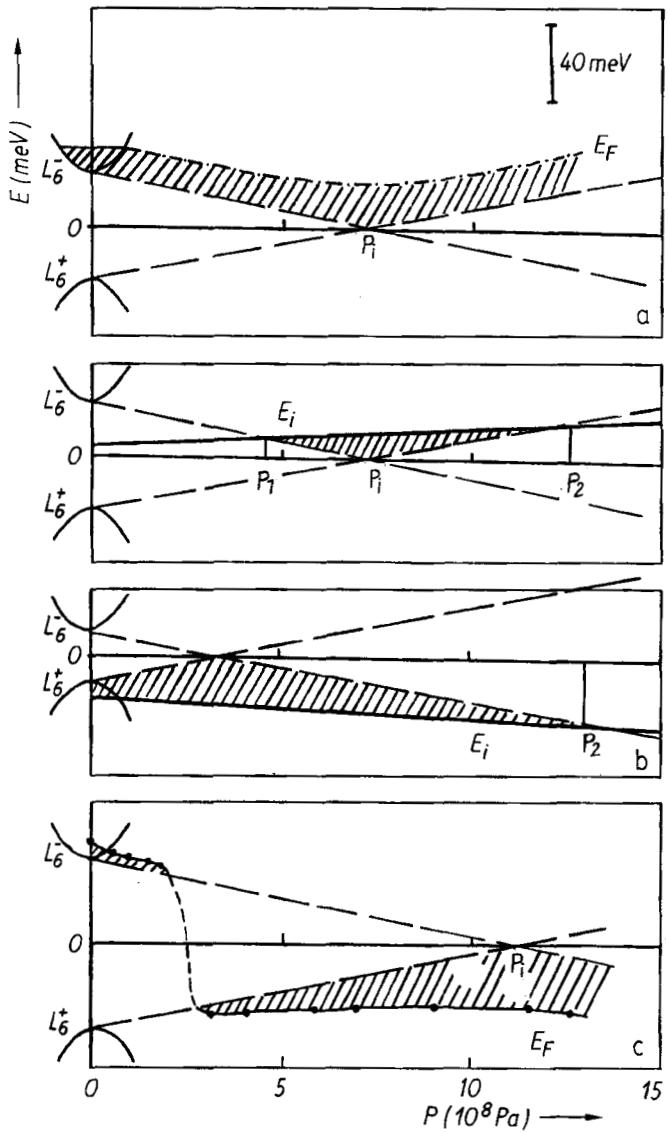

Fig. 4. The diagrams representing the reconstruction of the energy spectrum under the effect of pressure for: a) undoped $Pb_{0.75}Sn_{0.25}Te$, b) $Pb_{0.75}Sn_{0.25}Te$(In), c) $Pb_{0.70}Sn_{0.30}Te$(In), d) $Pb_{0.81}Sn_{0.19}Te$(Ga)

In PbTe(Cr) pressure also induces a change of the electron concentration [20]. The calculations show that this variation corresponds to the stable FL position relative to the middle of the gap.

In high-ohmic n-PbTe(Ga) crystals application of pressure results in the reduction of the activation energy of the conductivity and in the conversion of its type from n to p at $P \approx 10^9$ Pa [19]. A unique result has been obtained for $Pb_{1-x}Sn_xTe$(Ga) under hydrostatic pressure. In n-type samples (the FL seems to be not pinned) in a narrow pressure interval

the FL passes through the gap and enters the valence band [45] (see Fig. 4). Such a "jump" of the FL has been explained in terms of a pressure induced change of the charge state of the Ga atom in the crystal lattice. It has been supposed that even slight strains of the crystal lattice or maybe slight deviations from the equilibrium position of Ga atoms due to these strains change the charge state of Ga atoms and transform it from donor to neutral impurity. A similar situation has been observed in $Pb_{1-x}Ge_xTe(Ga)$ single crystals at cooling [46]. A rapid diminishing of the resistivity at a definite temperature depending on the alloy composition x has been attributed to the change of the charge state of Ga atoms due to the strain of the crystal lattice induced by the ferroelectric phase transition.

3.3 Energy spectrum of the MLTA in high magnetic fields

The effect of Fermi level pinning induces qualitative changes of the galvanomagnetic properties of the MLTA in the ultraquantum limit (UQL) of magnetic fields. The experimental observation of this phenomenon is possible if, first, the pinning really exists and, second, the UQL can be achieved. It means that the Fermi energy must be small enough. $Pb_{1-x}Sn_xTe(In)$ alloys appear to be nearly ideal systems for the experimental study of FL pinning in a magnetic field. Using the hydrostatic pressure as a tool that can tune the position of FL relative to the band edges it is possible to choose the desired initial state. One can choose the electron ($x < 0.22$) or hole ($x > 0.28$) type of conductivity, the direct ($P < P_i$) or inverse ($P > P_i$) region of the energy spectrum [48]. The dependence of Hall voltage on the magnetic field H is shown in Fig. 5 for an n-type $Pb_{1-x}Sn_xTe(In)$ alloy ($x = 0.25$) at various temperatures and pressures. It should be noted that at low temperature ($T < 20$ K) the processes of relaxation to the equilibrium state in these alloys are of long

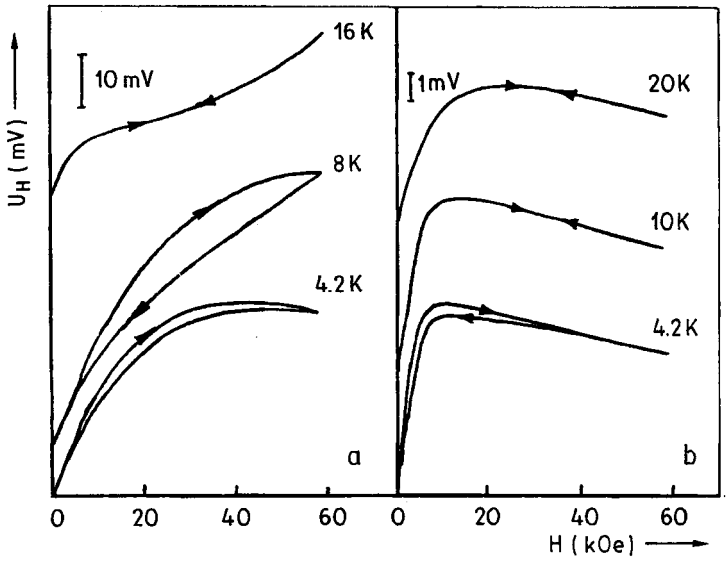

Fig. 5. Recorded $U_H(H)$ dependence for $Pb_{0.75}Sn_{0.25}Te(In)$ at various temperatures and pressures. Temperatures are indicated by the figures at the curves [48]; a) $P = 2.8 \times 10^8$ Pa $< P_1 < P_i$, b) $P_2 < P = 14 \times 10^8$ Pa

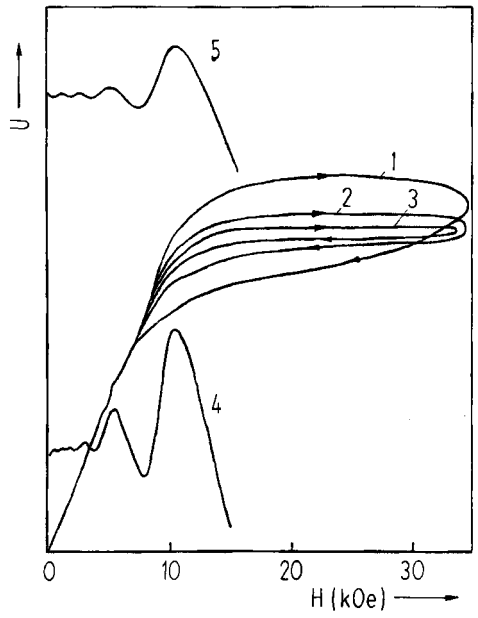

Fig. 6. Recorded curves of $U_H(H)$ with dH/dt = 15, 8, 4 kOe/min, (1) to (3), respectively, (4) magnetoresistance oscillations $\Delta\varrho(H)/\varrho_0$, (5) Hall voltage oscillations $\Delta U_H(H)/U_0$ with monotonous components of $\varrho(H)$ and $U_H(H)$ compensated, for $Pb_{0.70}Sn_{0.30}Te(In)$ at $P = 9.2 \times 10^8$ Pa, $T = 4.2$ K [48]

duration (see Section 4.1). But in this section we consider only the equilibrium state without any consideration of the way it has been reached.

The $U_H(H)$ curves are stationary in high fields at temperatures $T \approx 16$ to 20 K. This means that for every fixed field H the equilibrium value of U_H is reached during a time of $\tau \approx 1$ s.

In the vicinity of a certain definite value of the field $H = H_0$ a deviation from the linear dependence $U_H(H)$ is observed. In the metallic state ($P_1 < P < P_2$) this field equals the ultraquantum limit field H_{uql}, that corresponds to the crossing of the Fermi level by the 0^+ Landau level. The H_{uql} field can be estimated by means of Shubnikov-de Haas (SdH) measurements, since H_{uql} corresponds to the last extremum of the $\Delta\varrho(H)/\varrho_0$ oscillation curve. In these experiments the orientation of the magnetic field was $\boldsymbol{H} \parallel \langle 100 \rangle$. This configuration corresponds to the equivalent position of four isoenergetic ellipsoids relative to the vector $\boldsymbol{H}$. All the experiments described below have been performed in the same orientation. Fig. 6 represents the $U_H(H)$ curves (curve 3 is close to the stationary one) and the oscillating component of $\varrho(H)$ for the alloy with $x = 0.30$. In the dielectric state ($P < P_1$, $P > P_2$) the H_0 value lies in the range of 1 to 3 kOe.

The stationary $U_H(H)$ dependence significantly differs in the direct and inverse energy spectrum regions: when $P < P_i$, $U_H(H)$ is a slightly increasing function, and when $P > P_i$ it is a decreasing function of magnetic field $H > H_{uql}$. In the vicinity of P_i, U_H is practically independent of H at high fields $H > H_{uql}$. This behaviour was observed in both n- and p-type $Pb_{1-x}Sn_xTe$ alloys.

The results obtained in [49] show that the transformation of the energy spectrum of $Pb_{1-x}Sn_xTe$ alloys can be described by the two-band Kane model modified to account for the fact that the effective g-factor differs from 2. In this model the dispersion equation for electrons and holes in the L bands for $\boldsymbol{H} \parallel z$ is as follows [48]:

$$(E^2 - \tfrac{1}{4}E_g^2)/E_g = \hbar\omega_c(n + \tfrac{1}{2}) \pm \tfrac{1}{2}g\mu_B H + h^2k_z^2/2m_z, \tag{3.1}$$

where the energy E is calculated from the middle of the band gap E_g, $\omega_c = eH/m_c c$, m_c is the cyclotron mass, g the spectroscopic g-factor, m_z the effective mass in z-direction (parameters m_c, g, and m_z correspond to the band edges), and $\mu_B = eh/2m_0c$ is the Bohr magneton. For arbitrary z-direction this relation has different parameters for each of the ellipsoids, but if $\boldsymbol{H} \parallel z \parallel \langle 100 \rangle$ these parameters are equal. In the further consideration we

use rather simple equations corresponding to this model, though a more precise approach taking into account the Landau level broadening has been proposed in [50].

It can easily be shown that for degenerate statistics of charge carriers the ratio of the electron (or hole) concentration n_{uql} at $H > H_{uql}$ to that at $H = 0$ is given by [48]

$$\frac{n_{uql}(H)}{n_0} = \frac{3}{2}\frac{m_0\mu_B H E_g(\tilde{E}_F^2 - \frac{1}{4}E_g^2)^{1/2}}{m_c[(\tilde{E}_F^0)^2 - \frac{1}{4}E_g^2]^{3/2}}\left[1 - \frac{\mu_B H E_g \Delta}{\tilde{E}_F^2 - \frac{1}{4}E_g^2}\right]^{1/2}, \tag{3.2}$$

where $\Delta = (m_0/m_c)(1 - \tilde{g}/2)$ ($\tilde{g}$ is the effective g-factor), $\tilde{E}_F = (E_F + E_g/2)$ Fermi energy calculated from the middle of the gap. In the general case $\tilde{E}_F$ depends on H, and $\tilde{E}_F^0 = \tilde{E}_F(H = 0)$. For the undoped $Pb_{1-x}Sn_xTe$ alloys $n(H) = n_0 = \text{const}$, hence $n_{uql}/n_0 = 1$, and (3.2) describes the dependence $E_F(H)$. If the FL is pinned, $E_F(H)$ will be equal to E_i and (3.2) describes the dependence $n_{uql}(H)$.

The $n_{uql}(H)/n_0$ dependence for $H > H_{uql}$ is completely defined by the magnitude of the magnetic field and by the magnitude and sign of the parameter Δ. In essence, in the case of FL pinning (3.2) describes the magnetic field induced charge carrier transition between the E_i level and the L bands. This process originates from the following: (i) The electron (hole) density of states increases in a magnetic field, resulting in an increasing band capacity for every fixed energy interval; (ii) the band edges will move in a magnetic field relative to the E_i level.

Fig. 7a represents the spectrum of the $Pb_{1-x}Sn_xTe(In)$ alloy in zero magnetic field for $P_1 < P < P_i$. The change in the spectrum at $H > H_{uql}$ is shown in Fig. 7b for the case when the spin splitting of the Landau level is smaller than the orbital one ($\tilde{g} < 2$). Only the 0^- Landau level remains below the E_i level when $H > H_{uql}$. The parabola in Fig. 7b represents the quasi-continuous nature of the spectrum in the k_z direction. Occupied and vacant states are represented by filled and open dots. The transition process is shown schematically by arrows.

According to (3.2), n_{uql} increases linearly in a magnetic field when $\Delta = 0$ ($\tilde{g} = 2$) with the equilibrium magnitude of the Hall voltage given by

$$U_H(H) = \text{const}\frac{H}{n_{uql}(H)} \tag{3.3}$$

and does not depend on H.

When $\Delta > 0$ ($\tilde{g} < 2$), $n_{uql}(H)$ increases slowly at first, then passes through a maximum, and decreases.

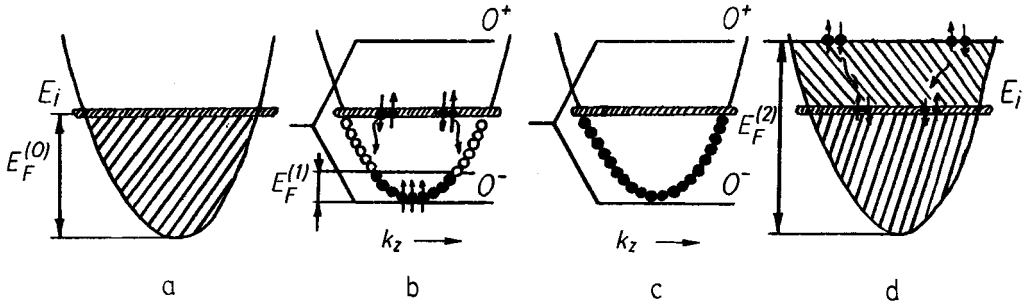

Fig. 7. The non-equilibrium metallic state cycle [13]

The experimentally obtained deviations from the linear $U_H(H)$ dependence in magnetic field and numerical calculations show that the Fermi level in $Pb_{1-x}Sn_xTe(In)$ alloys is pinned in a quantizing magnetic field. The rapid growth of $n_{uql}(H)$ is the main evidence for this conclusion ($n_{uql}(H)/n_0$ = (10 to 20) when H = 6 T) [48].

4. Non-Equilibrium States in the MLTA Induced by Magnetic Field and Illumination

In the previous part of the paper we have considered the stationary state of the MLTA. At low enough temperatures the kinetics of the relaxation to the equilibrium state after excitation by some external factor is a long-term process. For example, in $Pb_{1-x}Sn_xTe(In)$ the reduction of temperature to $T \leqq 20$ K results in the appearance of a hysteresis in the $U_H(H)$ curves (see Fig. 5 and 6) when the field is increased and then decreased at a finite rate ($\approx$10 kOe/min). It is connected with rather high direct (level–band) and inverse (band–level) transition times of non-equilibrium charge carriers [48, 51]. In the present section we will consider the long-term relaxation of galvanomagnetic parameters.

4.1 Non-equilibrium states in high magnetic field

It is convenient to start a detailed study of the corresponding phenomena from the consideration of the cycle by which a quasi-equilibrium metallic state with frozen Fermi surface is reached, as proposed in [13] for $Pb_{1-x}Sn_xTe(In)$ alloys. Let us return to Fig. 7, where energy diagrams are represented, and illustrate the following stages of the cycle:

1. $H = 0$, $T = 4.2$ K. The alloy is in the metallic state with Fermi energy E_F.

2. $T = 4.2$ K. As a magnetic field $H_i > H_{uql}$ is imposed, the energy spectrum transforms as shown in Fig. 7b. The density of states in the 0^- Landau level grows and the number of allowed states under the pinned FL increases. Since the process of the level–band transitions of electrons is of long duration, the quasi-FL at first falls down to $E_F^{(1)}$ and then slowly grows. In the limit that the characteristic time of the level–band transitions $\tau_1 \to \infty$, $E_F^{(1)}$ is determined by (3.2) where $n_{uql} = n_0$.

3. $H = H_i > H_{uql}$, the magnetic field magnitude being fixed. The sample is heated up to $T = 20$ K. During heating intense level–band transitions start and the 0^- Landau band is rapidly filled by electrons up to the E_i level. As the temperature is reduced, the equilibrium state of the system becomes frozen (Fig. 7c).

4. $T = 4.2$ K. The magnetic field is reduced to $H = 0$. Since the characteristic time τ_2 of the reverse band–level transitions is also long, the electron concentration in the conduction band decreases slowly relaxing to the equilibrium value. In the limit $\tau_2 \to \infty$ the quasi-FL position $E_F^{(2)}$ is determined by (3.2) where the n_0 value must be replaced by $n_{uql}(H_i)$ (Fig. 7d).

5. $H = 0$. The sample is heated to $T = 20$ K. Intense band–level transitions start and the Fermi level drops down to its initial position E_F. When the temperature is reduced, the system returns to its initial state at $T = 4.2$ K.

This cycle is reproducible.

Analysis of the $U_H(H)$ time dependence in a fixed field shows that the U_H relaxation cannot be described by a simple exponential law with a parameter $\tau_{1(2)}$. In order to describe quantitatively the dependence of the relaxation rate on x, P, and T, in [48] a characteristic parameter τ has been introduced. It has been defined as the time necessary for the non-equilibrium Hall voltage U_H, in a fixed magnetic field $H > H_{uql}$, to change from its initial value by a factor of e. The comparison of τ determined in such a way for alloys

with different x-values shows that for the level–band transitions τ_1 approaches several ten hours in the alloy with $x = 0.20$ and decreases to 0.5 h in the alloy with $x = 0.30$ at $T = 4.2$ K, $P = 10^5$ Pa, and $H = 6$ T. For all the alloys with x from 0.20 to 0.30 an increase of pressure up to 15×10^8 Pa causes a considerable decrease of τ_1 to ≈ 1 s at $T = 4.2$ K. A sharp reduction of τ_1 to values below 1 s at $P = 10^5$ Pa in all the alloys can be obtained by increasing the temperature up to $T_c \approx 20$ K.

The existence of the long-term relaxation process caused by charge carrier transitions between the E_i level and the allowed bands indicates that impurity and band states in $Pb_{1-x}Sn_xTe$(In) alloys are separated by a barrier W. The authors of [48, 51] have estimated the W-value as (20 to 40) meV using the equation for a simple activation process (10 K $< T <$ 25 K),

$$\tau = \tau_0 \exp(W/kT). \tag{4.1}$$

The deviations from the exponential law in the experimentally observed relaxations may be connected with a large deviation from the equilibrium state (as well as with other factors). According to (4.1) the relaxation time τ would increase up to $\approx 10^{30}$ s with a decrease of temperature to 4.2 K with $W \approx 30$ meV and $\tau_0 \approx 10^{-8}$ s. This value lies far beyond the experimentally obtained τ_1 value. It may be due to the coexistence of activation and tunnelling mechanisms in the relaxation process at low temperatures.

The analysis of experimental data shows that τ_1 for fixed $H > H_{uql}$ and x, P, T parameters exceeds the corresponding value of τ_2 for the inverse transition. It is illustrated in Fig. 5: the hysteresis in the $U_H(H)$ dependence recorded at various values of $\partial H/\partial t$ is observed only in stronger fields, and in weak fields the $U_H(H)$ curves practically coincide. In this example the relation $\tau_2 < \tau_1$ can be observed because both τ_1 and τ_2 values decrease with increasing x and P.

It should be pointed out that the processes of level–band and band–level transitions are physically different. The application of a quantizing magnetic field induces the spin polarization of charge carriers; the energy spectrum becomes one-dimensional. According to the model (see the next section of this paper) in $Pb_{1-x}Sn_xTe$(In) alloys some of the impurity centres are occupied by two electrons with oppositely directed spins, other centres being empty. The level–band transitions thus can be accompanied by a change of the spin direction (see Fig. 7b). It is obvious that the relaxation occurs without spin-flip during the band–level transitions because of the spin degeneracy of the conduction band (see Fig. 7d).

4.2 Non-equilibrium processes under IR-illumination

In the present section of the paper infrared illumination will be considered as a disturbing parameter. In comparison with other factors it possesses the widest range of possible excitation levels. The non-equilibrium states induced in this way have been investigated for $Pb_{1-x}Sn_xTe$(In) alloys in [52 to 59] and for PbTe(Ga) in [27, 31, 33, 54, 59 to 62].

The high sensitivity of $Pb_{1-x}Sn_xTe$(In) and PbTe(Ga) samples to the background radiation results in additional requirements to the experimental procedure. The authors of [53] used a vacuum metallic chamber cooled by liquid helium for the photoconductivity measurements. The construction of the chamber provided practically complete screening of the sample from the background thermal radiation. A carbon resistor heated by electric current or a light-emitting diode (LED) is used as source of infrared radiation. The sample

temperature (T) and the temperature of the carbon resistor (T^*) were controlled by thermocouples. The measurements were performed in electric fields less than 0.2 V/cm.

The typical temperature dependences of the sample resistivity ϱ measured in the dark and under infrared illumination in $Pb_{0.75}Sn_{0.25}Te(In)$ and PbTe(Ga) alloys are shown in Fig. 2. The maxima on curves 1′, 2′ at the temperature $T = T_c \approx 20$ K for $Pb_{0.75}Sn_{0.25}Te(In)$ and $T = T_c \approx 80$ K for PbTe(Ga) are due to the appearance of photoconductivity [54]: the resistivities in the dark (ϱ_0) and under illumination (ϱ') at $T < T_c$ differ by several orders of magnitude. No noticeable correlation between T_c and x in $Pb_{1-x}Sn_xTe(In)$ alloys has been found. The Hall mobility of free carriers is of order of 10^4 cm^2/Vs and remains approximately constant for $T \leqq T_c$ in all samples studied. It should be noted that high photoconductivity is observed in both n-type ($x \leqq 0.25$) and p-type ($x \geqq 0.26$) $Pb_{1-x}Sn_xTe(In)$ alloys in the dielectric state ($0.22 \leqq x \leqq 0.28$) as well as in the metallic one ($x \leqq 0.22$, $x \geqq 0.28$).

An effective method for investigating the photoconductivity in $Pb_{1-x}Sn_xTe(In)$ alloys in the metallic state is the registration of Shubnikov-de Haas oscillations of non-equilibrium carriers at different excitation levels [48]. The observation of this effect becomes possible due to the existence of a barrier which prevents the fast recombination of non-equilibrium charge carriers and gives an opportunity to fix the position of the quasi-Fermi level at some definite value for every temperature of the excitation source. The same reason permits to observe the dielectric–metal transition induced by the IR-radiation, which is accompanied by the appearance of SdH oscillations in $Pb_{1-x}Sn_xTe(In)$ alloys being initially in the dielectric state. The magnetoresistance derivatives $\partial\varrho/\partial H$ in $Pb_{0.78}Sn_{0.22}Te(In)$ for the quasi-stationary case at different levels of excitation are presented in Fig. 8. If the temperature of the illumination source is fixed, the oscillation frequency determined by the charge carrier concentration begins to increase slowly and reaches the quasi-stationary value corresponding to equal rates of generation and recombination processes. If the infrared illumination is switched off, the oscillation frequency starts to decrease and the size of the quasi-Fermi surface slowly diminishes, too. The experimental investigations show that the values of the non-equilibrium free carrier concentra-

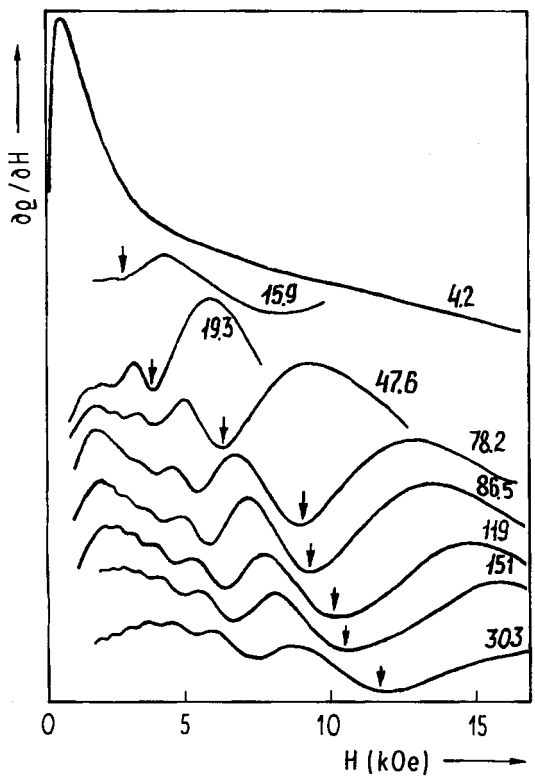

Fig. 8. Recorded $\partial\varrho/\partial H$ oscillations for $Pb_{0.78}Sn_{0.22}Te(In)$ alloy at 4.2 K under irradiation. Figures at the curves are T^* in K; $T = 4.2$ K [53]

tion Δn induced by the illumination achieve 10^{17} to 10^{18} cm^{-3}. These high values of Δn cannot be obtained in quantizing magnetic fields.

A detailed investigation of the conductivity relaxation to its equilibrium value σ_{st} after the illumination was switched off was performed for $Pb_{1-x}Sn_xTe$(In) alloys by several research groups [53, 55 to 58]. The relaxations appear to be rather complicated, and the majority of authors have found the character of the observed $\sigma(t)$ dependences to be non-exponential. For the interpretation of the experimental results different approaches have been used. In [57] the dependence $\sigma(t)$ has been fitted by two exponentials with different arguments. In a later paper [58] the authors proposed a phenomenological equation for the relaxation of the photoconductivity in an exponential form, but the relaxation time itself was time-dependent as a result of the quasi-FL movement during the relaxation process. In [55] the persistent photoconductivity relaxation has been found to obey a logarithmic law. In [53] the relaxation curves have been approximated by a power law. Such discrepancies seem to be connected with the difficulties to describe the whole relaxation curve by a simple equation. Maybe the choice of various regions of the curve by different authors gives rise to the appearance of a variety of interpretation possibilities. Another difficulty in the investigation of the relaxation process is a noticeable dependence of the relaxation parameters on the excitation level. It should be noted that the shape of the relaxation curves depends also on the In content, N_{In}, in the investigated alloys [63].

A study of the relaxation process in $Pb_{1-x}Sn_xTe$(In) alloys with different composition x has been performed in [53]. It has been found that $\sigma(t \to \infty)$ at a fixed T^* saturates towards $\sigma_{st}(T^*)$. At a carbon resistor IR-source temperature $T^* \geqq 100$ K $\sigma_{st}(T^*)$ does not change. The saturation level $\sigma_{st}(T^*)$ strongly depends on x. When x rises starting from 0.22, σ_{st} at first slowly decreases attaining a minimum at $x = 0.26$ and then begins to increase. At this composition, $x = 0.26$, the Fermi level passes through the middle of the band gap (see Fig. 3) and the conductivity type changes from electron to hole type. The decrease of σ_{st} to the equilibrium value after the illumination has been switched off can be described by a power function $(\sigma - \sigma_0)/\sigma_0 = At^{-\beta}$ for all alloys investigated and for different levels of excitation (σ_0 is the conductivity value in the dark). It has been found that as the temperature T^* rises from 20 to 250 K, the parameter β decreases from ≈ 2 to 0.45, 0.7, 0.3 for $x = 0.25$, 0.27, 0.28, respectively. At a fixed T^* the parameter β reaches its maximum value at $x = 0.26$. For this composition the relaxation times of the non-equilibrium charge carriers reach a minimum ($\tau < 0.1$ s even at $T = 4.2$ K). The parameter β also seems to depend on the σ_{st} value, which is determined by the excitation level.

The kinetics of photoconductivity in the high-ohmic PbTe(Ga) crystals is rather complicated. Noticeable photoconductivity is observed at $T < T_c \approx 80$ K (Fig. 2). At $T = 77$ K the value of the lifetime τ_h of non-equilibrium holes is $\tau_h < 10^{-8}$ s and that of the electrons is $\approx 10^{-3}$ s [61, 62]. A decrease of temperature results in the appearance of at least two distinct regions in the $\sigma(t)$ curves. A fast process occurs immediately after switching off the illumination. At $T = 4.2$ the corresponding time is $\approx 10^{-2}$ s. A long-duration process follows the fast one and its relaxation time is $> 10^5$ s (see Fig. 9). The balance between the concentrations of non-equilibrium charge carriers participating in each process depends on the duration and the intensity of the illumination.

The long-term processes in the MLTA considered above are qualitatively different from the relaxation of non-equilibrium charge carriers in inhomogeneous semiconductors. The main evidence for this conclusion is the observation of the slowly diminishing Fermi surface in the metallic state of the alloys accompanied by a change of the period of SdH oscillations.

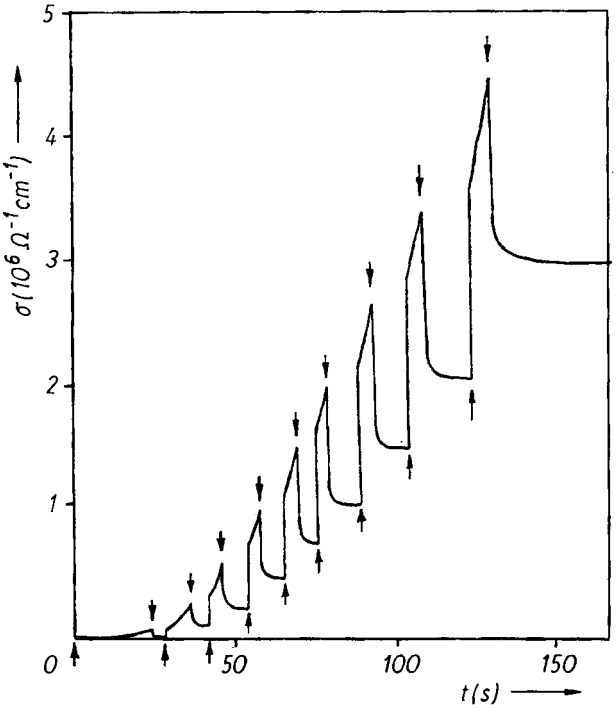

Fig. 9. Kinetics of rise and reduction of photoconductivity for PbTe(Ga) excited by an LED, $\lambda = 1$ μm, $T = 4.2$ K. The arrows show illumination switching on and off [31]

5. Theoretical Models of the Defects Forming the Long-Living States in PbTe-Based Materials

The analysis of the experimental data performed in the preceding section led to the conclusion that the doping of $Pb_{1-x}Sn_xTe$ with In and some other impurities caused the formation of long-living local and quasi-local electron states. It is not clear, however, whether these states are introduced by the impurity atoms themselves or whether doping favours the appearance of another kind of defects which in turn form the quasi-local states. The second possibility is supported by the fact that the observed density of quasi-local states may be very different from the impurity concentration [64] (see details in Section 7.1).

In the absence of detailed information about the structure of the defect forming the quasi-local state its theoretical models were based mainly upon phenomenological consideration. Generally, in order to slow down the carrier transition rate between an impurity and a band a barrier should be overcome in the transition process. The barrier separates the regions where the wave functions of free and localized states have non-zero values, hence their overlap becomes very small and so does the transition matrix element. Probably, the most obvious example of this kind is the Coulomb barrier of a many-electron centre that slows down the carrier trapping [66]. However, the Coulomb interaction is inefficient in $Pb_{1-x}Sn_xTe$(In) alloys because of the very high value of their dielectric constant (see Table 1), so it cannot form a noticeable barrier. Hence the barrier can appear only due to short-range forces. As barriers of this kind are very thin (of the order of the lattice period), electrons can penetrate them easily, so at first sight the short-range barriers cannot be the origin of a long-term relaxation. But the situation changes completely if the transition is

not entirely electronic but involves also a lattice distortion due to the electron–phonon interaction at the centre. In other words, let us consider an electron transition that is accompanied by impurity movement, i.e. a change of the impurity position in the unit cell, which is a common feature of deep traps [67]. As the mass of the impurity is much greater than the electron mass, even a thin short-range barrier can be an almost unsurmountable obstacle for the centre movement and hence for the transition as a whole.

This idea that has been first introduced by Gurney and Mott in 1939 [68] in similar context and is the base of practically all models for the formation of defect states in $Pb_{1-x}Sn_xTe$ [69 to 76]. Approaches used by different authors differ mainly in the assumptions on the structure of the centre and also in treatment of the electron–lattice coupling mechanism. The choice of an adequate model is not easy, first, because of the insufficient experimental information about the structure of the centre, and second, because predictions of many different approaches are similar and often do not differ in their physical content but rather in the details. In their more elaborate versions [72 to 74] the models of the doping-induced defect in $Pb_{1-x}Sn_xTe$ are very similar to the well-known Anderson model of the negative-U centre [76]. The two-electron nature of the ground state of the centre is supported by the absence of the paramagnetic resonance signal of the defects.

Fig. 10 shows the energy level diagram of the defect according to [73, 74], and the corresponding analytical expression for the energy of the centre having captured n electrons ($n = 0$, 1, or 2) is

$$\varepsilon_n = \Delta^2/(2\Delta_0) + (\varepsilon_0 - \Delta)\, n + U_n, \tag{5.1}$$

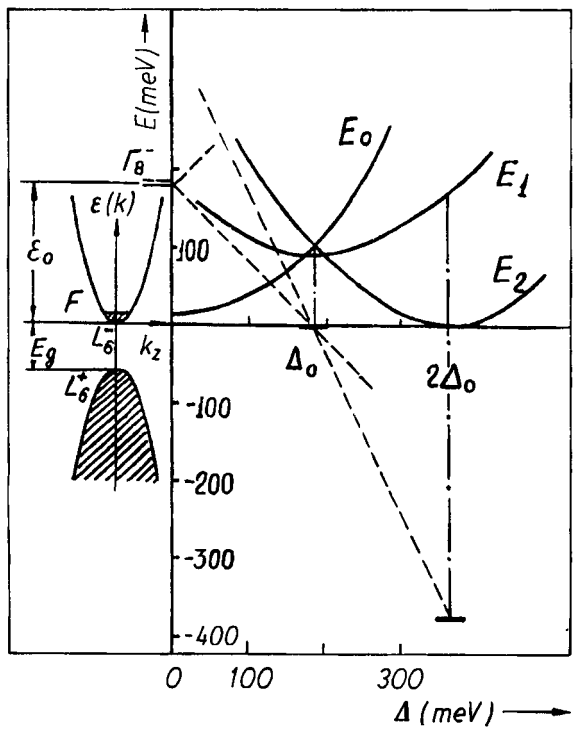

Fig. 10. The energy level diagram of the defect vs. configuration coordinate Δ; $\varepsilon_0 = 175$ meV, $\Delta_0 = 180$ meV

where Δ is the configuration coordinate measured in energy units so that Δ equals the energy shift of the one-electron level of the defect which is linear in the deformation, Δ_0 is the parameter determining the strength of the electron–phonon interaction at the centre, ε_0 is the energy position of the empty level of the centre (both Δ_0 and ε_0 depend upon the alloy composition, see later), $U_n = U\delta_{n2}$ is the energy of the Coulomb repulsion of two electrons at the centre, δ_{ij} being the Kronecker symbol. Here $U = e^2/\varkappa r \approx 10$ meV, $r \approx 1$ nm is the radius of the quasi-localized electron state, and $\varkappa \approx 180$ is the value of the static dielectric constant reduced due to the effect of spatial dispersion [73]. It is worth noting that because of the large dielectric constant the electron–electron interaction at the centre is small as compared to the energy gain due to electron–phonon interaction ($\Delta_0 \approx 100$ meV, see later), so the defect is a centre with negative correlation energy.

This model was originally introduced in [73] for the energy level structure of the chalcogen vacancy in $Pb_{1-x}Sn_xTe$ and was based on the detailed calculation of its spectrum. Being treated as a phenomenological one, this model with parameters determined from experiment proved to be useful for the interpretation of different experimental data concerning the In doping-induced defect.

The dependence of Δ_0 and ε_0 (in eV) upon alloy composition x was found in [65] for the interval $0.12 < x < 0.25$:

$$\varepsilon_0(x) = 0.43 - 1.2x\,, \qquad \Delta_0(x) = 0.32 - 0.65x\,,$$

where ε_0 is measured from the bottom of the conduction band.

For different n-values the functions $\varepsilon_n(\Delta)$ represent the energy of the centre occupied by n electrons. It is often more convenient to consider the energy of a system consisting of the centre with n electrons and of $(2 - n)$ free electrons in the band. The full number of particles in this system remains unchanged independently of n, hence the energies of the system states can be compared directly, for example, in thermodynamic calculations. Denoting the energy levels of this system by E_n, one obtains

$$E_n(\Delta) = \varepsilon_n(\Delta) + (2 - n)\,E_F\,, \tag{5.2}$$

where E_F is the Fermi energy.

From (5.2) one can easily see, in particular, that the condition of Fermi level pinning

$$E_{0\,\min} = E_{2\,\min}\,,$$

where the subscript min stands for the equilibrium (minimum in Δ) energy value, reduces to

$$2E_F = \varepsilon_{2\,\min} = 2(\varepsilon_0 - \Delta_0) + U\,. \tag{5.3}$$

The two-electron nature of the defect ground state is reflected clearly in this equation.

Using (5.2) and (5.1) one can calculate the heights of the barriers that the system has to overcome either thermally or by tunnelling in order to change the charge state of the centre. Finding the intersection points of the $E_n(\Delta)$ and $E_{n-1}(\Delta)$ curves one obtains the following expressions for W_{ij}, the barrier height for the transition from the state with i electrons bound at the centre to the state with j bound electrons ($|i - j| = 1$ for one-electron transitions):

$$W_{01} = \frac{(\varepsilon_0 - E_F)^2}{2\Delta_0}\,, \qquad W_{10} = \frac{(\varepsilon_0 - \Delta_0 - E_F)^2}{2\Delta_0}\,,$$

$$W_{12} = \frac{(\varepsilon_0 - \Delta_0 + U - E_F)^2}{2\Delta_0}\,, \qquad W_{21} = \frac{(\varepsilon_0 - 2\Delta_0 + U - E_F)^2}{2\Delta_0}\,.$$

Because usually ε_0 and Δ_0 are significantly larger than U and E_F, W_{01} and W_{21} are larger than the other two barriers, the corresponding transitions are much slower than others. In particular, the large value of W_{21} for the barrier that separates the lower two-electron state of the defect from its excited one-electron state may lead to the long-living character of the lower state when it lies on the background of a band and hence is a quasi-localized one. Indeed, the barrier complicates strongly the electron transition from this state at low temperatures. In some cases the excited state of the centre may be also long-living, and we will often call it metastable state to distinguish it from the ground state. However, the reader should bear in mind that the lifetime of this state depends upon alloy composition, temperature, and other parameters and hence may vary (see Sections 7, 8).

6. Carrier Kinetics in the Modified Lead Telluride Alloys in High Electric Field

Bulk non-equilibrium electron properties of doped $Pb_{1-x}Sn_xTe$ alloys as well as of any other semiconductor depend upon the electron energy spectrum of the material and the carrier scattering processes in it.

From the point of view of the transport phenomena the main features of the band spectrum of $Pb_{1-x}Sn_xTe$ are a small value of the energy gap E_g, a significant non-parabolicity of $\varepsilon_c(p)$ and $\varepsilon_v(p)$, the electron and hole energy dispersion laws, and the symmetry of the spectrum so that $\varepsilon_c(p) \approx -\varepsilon_v(p)$ if the energy is measured from the middle of the gap. Extrema of both the bands are situated in the eight L points of the Brillouin zone. The constant energy surfaces near extrema are close in shape to prolate spheroids. The simple formulae for the energy spectrum parameters are represented in Table 1; more complicated and precise expressions can be found in [3].

The obvious consequence of the symmetry of the spectrum is that electron and hole mobilities do not differ significantly.

6.1 Carrier scattering mechanisms in $Pb_{1-x}Sn_xTe$

Let us now turn to the carrier scattering processes in $Pb_{1-x}Sn_xTe$ alloys. As the alloys are heavily doped materials, one could suppose that impurity scattering should be important. However, the Coulomb scattering of electrons by ionized impurities is strongly suppressed due to the very large value of the dielectric constant $\varkappa_0 \approx 450$ to 2000 [77] in $Pb_{1-x}Sn_xTe$ so that the scattering can manifest itself only at temperatures less than 77 K at the highest doping levels ($N_i \geqq 10^{18}$ to 10^{19} cm^{-3}). Nevertheless, the impurities that form quasi-local (resonant) electron levels not far from the band edge, as, for example, Tl atoms do, can influence the carrier mobility very significantly because of resonant scattering [78, 79] of electrons by these states. It is a very effective scattering process for carriers with energy nearly equal to ε_0, the energy of the resonant level. The resonant scattering cross-section has the form [78]

$$\sigma(\varepsilon) = \frac{\pi}{k^2} \frac{\gamma^2}{(\varepsilon - \varepsilon_0)^2 + \gamma^2/4}, \tag{4.1}$$

where k and ε are the carrier wave number and energy, respectively, and γ is the width of the resonant level that is connected with the lifetime of the quasi-local state τ so that $\gamma \sim h/\tau$. Hence $\sigma_{max} = \sigma(\varepsilon \approx \varepsilon_0) = 4\pi/k^2 \sim \lambda^2$ where λ is de Broglie wavelength of the carrier so that σ can be large, especially if ε_0 and hence k are small. The resonant scattering can lead to a large mobility decrease when the Fermi level is in the vicinity of the quasi-local

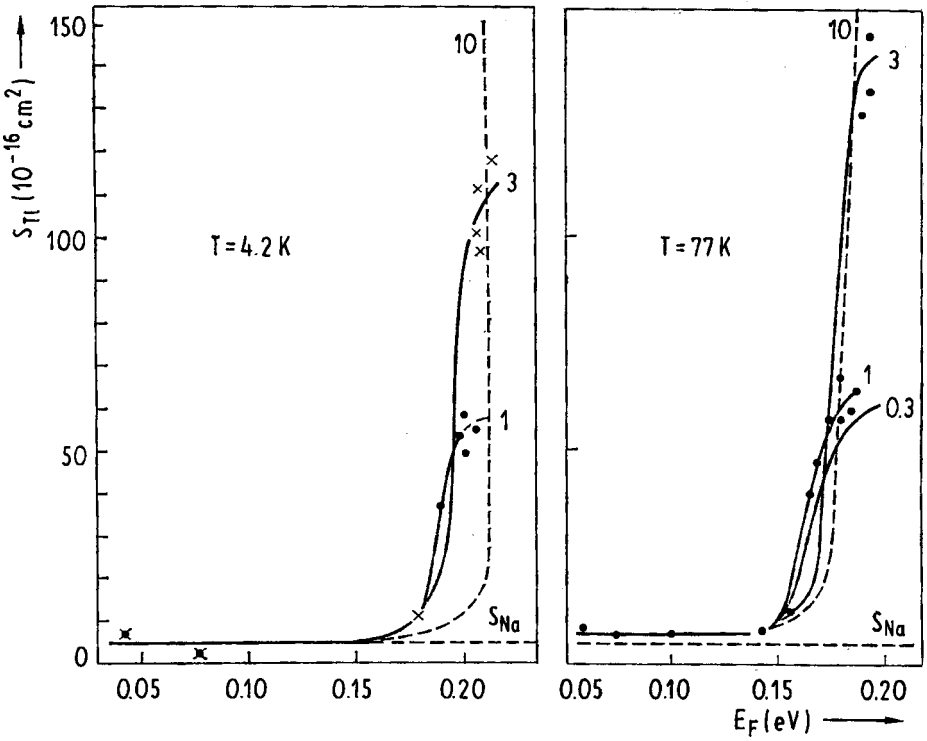

Fig. 11. Cross-section S_{Tl} vs. Fermi energy E_F for the resonant scattering of light holes in PbTe(Tl) [8]. Lines show the calculated $S_{Tl}(E_F)$ dependence for different ratios of mobilities of heavy and light holes: 0.3, 1, 3, 10. The cross-section S_{Na} for scattering by Na impurities is also shown

level. This effect has been observed [8] in PbTe doped with Tl (Fig. 11). In these experiments the Fermi energy was varied by changing the level of doping with Tl. It is important that no mobility decrease was observed at a similar hole concentration produced by "ordinary" impurities.

In $Pb_{1-x}Sn_xTe$(In) this effect was not observed.[2]) As we will see later the possible reason for this difference may be the different widths of Tl and In levels.

Even if the core potential of an impurity or defect cannot form a resonant level as is the case for the great majority of them [80] it still can influence carrier motion, but the corresponding cross-section is small. However, the small values of the cross-section can be compensated by the high concentration of scattering centres. An important example is the substitutional atom. The corresponding scattering mechanism is called the alloy scattering. It was shown to have an effect on the ohmic [81] and hot electron [82] transport in $Pb_{1-x}Sn_xTe$.

The phonon scattering processes look more ordinary. Three of them play an important role in this material, namely, DA, LO, and intervalley scattering [77, 82 to 87]. So the total number of scattering mechanisms equals five or six (the resonant scattering may be present

[2]) Indeed, many authors did not observe the resonant scattering in $Pb_{1-x}Sn_xTe$(In). However, in [172] the results of galvanomagnetic measurements were interpreted under the assumption of resonant scattering of holes by the In level.

or not). Each of them has its own specific dependence of its rate on the electron energy, lattice temperature, carrier and impurity concentration, alloy composition, etc. [88 to 90]. There is no simple rule to find out which process is the most important one under given conditions, and usually it is necessary to take several of them into account to obtain a correct description of the carrier transport even in the ohmic region [84, 86, 87, 91], and the situation becomes more complicated under hot electron conditions [82, 85, 92]. As a general tendency, at low carrier energy ε, i.e. less than the Debye temperature, the carrier mobility is dominated by DA and ionized impurity scattering. When ε is of order of the Debye temperature optical and intervalley phonon scatterings usually play the major role, and for the highest electron energies the DA phonon interaction becomes the most important scattering process because its probability increases most rapidly when the carrier energy is raised. It is not easy to point out the energy interval that is most favorable for the manifestation of alloy scattering because the energy dependence of the neutral centre cross-section depends on the nature of the defect and can have different forms [93, 94]. It is not clear whether the existing models are suitable for the description of the carrier interaction with substituting atoms in $Pb_{1-x}Sn_xTe$. In the simplest approach the slow particle scattering by a short-range potential is described by a constant cross-section [78] so that the energy dependence of the alloy scattering probability is the same as that of the DA phonon scattering. In contrast with the DA interaction the alloy scattering is temperature independent so it can be important at low temperatures when the efficiency of phonon scattering is reduced.

The parameters that describe the carrier scattering processes in $Pb_{1-x}Sn_xTe$ are summarized in Table 3. However, the electron–phonon and electron–defect interaction constants are not known precisely. For example, the values of the deformation potential constant for the DA interaction obtained by different authors differ significantly covering the interval 12 to 25 eV [84, 95] and even the value of 40 eV was sometimes used [86]. The value of the intervalley deformation potential constant in Table 3 was taken in [82, 85] simply equal to that for Ge. So one should treat these values rather as reasonable estimates than as strictly established data.

Table 3
Carrier scattering parameters in $Pb_{1-x}Sn_xTe$

static dielectric constant, $\varkappa_0$	450 to 2000 [77] $10^4/\varkappa_0 = 6.4 - 15x$, $0 < x < 0.35$ [120]
high frequency dielectric constant	37 [77] 38.4 [85]
optical phonon energy	$Pb_{0.8}Sn_{0.2}Te$: 14.2 meV [82] PbTe: 13.6 meV [85]
intervalley phonon energy	10.9 meV [82]
Debye temperature	$Pb_{0.8}Sn_{0.2}Te$: 126 K [83] PbTe: 160 K [83]
average acoustic deformation potential	12 to 25 eV [95, 84]
average L–L intervalley deformation potential	1.6×10^8 eV/cm [82]
average L–W intervalley deformation potential	2×10^8 eV/cm [82]
alloy scattering potential	0.15 eV [82]
sound velocity	3×10^5 cm/s [85]
mass density	7.9 to 8.2 g/cm^3 [82, 83]

The following examples can give some impression of the carrier mobility μ in the alloys: for $Pb_{1-x}Sn_xTe$ with $x = 0.17$ $\mu_{77K} \approx (2 \text{ to } 3) \times 10^5$ cm^2/Vs, μ_{300K} being an order of magnitude smaller [83], and for high quality epitaxial PbTe films $\mu_{4.2K} \approx 8 \times 10^6$ cm^2/Vs [120].

6.2 Hot electron phenomena in $Pb_{1-x}Sn_xTe$; theory

Let us now turn to the theoretical consideration of the hot electron phenomena in $Pb_{1-x}Sn_xTe$. The warm electron coefficient has been calculated in [86] taking into account the DA and LO phonon scattering. It was shown that the coefficient changed its sign from negative to positive as the lattice temperature was raised above the Debye temperature so that the $I-U$ curves were sublinear at $T_0 < \theta_D$ and superlinear at higher temperatures.

The calculations of the $I-U$ curves in high electric fields up to 3 kV/cm were performed in [85] for PbTe at $T_0 = 77$ K. The Monte Carlo simulation was used and DA, LO, and intervalley phonon scattering was taken into account. As T_0 was less than θ_D, sublinear $I-U$ curves were obtained in agreement with the results of [86]. The drift velocity value was equal to $(2.5 \text{ to } 3) \times 10^7$ cm/s at $E = 3$ kV/cm, the larger figure corresponding to the field parallel to the $\langle 100 \rangle$ direction and the smaller one to $\langle 110 \rangle$.

In these papers the carrier transport within only one band was considered and the possibility of interband carrier transitions was neglected. There are two most important channels of interband transitions, namely, impact ionization and transitions to the nearest higher extrema of the bands. These processes can influence the high field kinetics.

The effect of the interband impact ionization causing an increase of carrier concentration (i.e., interband breakdown) was detected in the early high field experiments in lead chalcogenides [96, 97]. A theoretical investigation of hot electron and hole transport under impact ionization conditions when the carrier concentrations depend on the electric field was performed in [98, 99]. The approach used there was based on the assumption that the carrier distributions could be described by Fermi functions, because the carrier density was high due to the interband breakdown, and that the main carrier recombination process was the Auger one because of the high concentration of electrons and holes and the small E_g value. As the breakdown effect was more prominent at low temperatures, DA phonon, ionized impurity, and electron–hole scattering processes were taken into account as well as the complicated band structure of $Pb_{1-x}Sn_xTe$ [99]. The calculated $I-U$ curves under impact ionization conditions showed a rapid current increase when the field was raised in the post-breakdown region, but no S-type negative differential conductivity (NDC) was found that had been observed in the experiments [96].

The influence of the possibility of electron transfer to a higher extremum in the conduction band on the hot electron phenomena in n-$Pb_{1-x}Sn_xTe$ was investigated in [92, 82]. It was shown that under appropriate choice of the effective mass in this so-called W extremum (about $0.5m_0$) and of the deformation potential constant value for the L–W scattering (see Table 3) these transitions could lead to the appearance of N-shaped $I-U$ curves due to the Gunn instability.

Let us now consider the effect of the quasi-local impurity or defect states on the non-equilibrium electron phenomena [100 to 102]. As these states are not very common in semiconductors we will do it in more detail.

The impurity centres producing resonant states affect strongly the electron transport. First, the electron scattering by these impurities has resonant nature. Its cross-section in

the maximum is large (see above). So the resonant impurities can influence significantly the carrier mobility. Second, the specific feature of the resonant scattering is an anomalously long carrier–centre interaction time. The collision duration is determined in this case not by the time of flight $\tau_f \sim a/v$ of the electron having velocity v through the effective range a of the impurity potential, but by the lifetime τ of the resonant impurity state [103]. As a rule, $\tau \gg \tau_f$. Moreover, for long-living resonant states it may happen that τ becomes greater than τ_p, the electron momentum relaxation time. The Boltzmann equation cannot be used for the description of the carrier kinetics in this case [101] because the equation is valid only when the collision duration is small as compared to τ_p [104]. So the problem arises to describe the electron transport in a semiconductor doped with long-living resonant impurities.

Physically, the problem connected with the long collision time is the following. The carrier spending a long time at the centre does not contribute to the current during this time. So the effect of the electron–resonant centre interaction on the transport is not only the carrier scattering as it is assumed in the Boltzmann equation. An additional effect arising here is the free electron concentration reduction due to their residence at the impurities. We want to stress that the described effect of the band electron concentration decrease is caused exclusively by the coherent and elastic process of resonant scattering itself. Quantum-mechanically, the effect in question is connected with the large wave function amplitude at the resonant scattering centre which is much greater than the electron wave amplitude far from the impurity.

Of course, inelastic processes can also limit the time an electron spends at the resonance centre. For example, the carrier occupying the impurity can absorb a phonon, or another electron can knock it out of the centre. The case when the inelastic capture and release times are much less than τ is relatively simple [100, 101]. One can neglect the quasi-stationary nature of the level and treat it as stable and local. Hence the carrier kinetics can be described by the usual kinetic equation taking into account these local levels, the band, and inelastic carrier transitions between them. If the level is situated in the band above the equilibrium FL position, so that only hot particles can effectively interact with it, then the possibility of hot electron transitions to impurity states can lead to N-shaped $I-U$ curves [100] due to the free carrier concentration decrease in high fields. The situation is somewhat similar to that in semiconductors doped by negatively charged impurities [105]. The NDC is entirely a concentration effect here, and the resonant scattering does not manifest itself because the carrier exchange between the centres and the band is controlled by inelastic collisions that destroy the coherence necessary for the formation of the typical resonant cross-section.

The opposite situation takes place when the lifetime of the resonant state is small as compared to the momentum relaxation time. In this case carriers spend almost all their time in free motion and the decrease of the band electron concentration due to carrier residence at the centres is negligible, as it is for any "ordinary" scattering mechanism. So the particle interaction with the resonant centres reduces to the resonant scattering only [101]. The Boltzmann equation is valid for the description of the carrier transport. The calculations [101, 106] showed that resonant scattering had a large effect on the conductivity and other kinetic coefficients only if the Fermi energy nearly coincided with the resonant level and the electron temperature did not exceed γ, the resonant level width, so that most part of the carriers were influenced by the resonant scattering. Consequently, in the hot carrier kinetics the resonant scattering generally does not manifest itself as clear as in ohmic conditions because the energy width of the hot distribution is larger and hence a smaller

fraction of carriers can interact with the resonant centres. However, the possibility of S-shaped $I-U$ curves was predicted [101] for semiconductor with short-living quasi-local levels ($\tau \ll \tau_p$) lying above the equilibrium carrier energy ($\varepsilon_0 \gg E_F, T_0$) in case when non-resonant electron scattering is due to ionized impurity interaction. The instability can take place due to the fast increase of the electron mobility when the carrier energy is raised above the resonant energy where the resonant scattering cross-section decreases rapidly.

The theory becomes more complicated in the intermediate case when both the resonant scattering and the electron residence at the resonant centres are important [102, 147]. It can happen if the resonance lifetime is comparable with or greater than the momentum relaxation time but still remains much less than the time of inelastic carrier release from the centre. In this situation the resonant scattering process is not influenced by inelastic collisions and hence the cross-section has its sharp resonant form (cf. (6.1)). As the free time is comparable with or less than τ that determines the time an electron remains at the centre during the resonant scattering [103], a particle having energy near the resonant value spends a significant or even most part of time at a resonant scattering centre and hence the concentration of free carriers in the band decreases. This effect is similar to that in case of extremely narrow quasi-local levels [100] (see above) but the electron density reduction is connected here solely with the coherent and elastic resonant scattering process. Of course, the concentration decrease will again result in N-shaped $I-U$ curves if the level is high enough in the band, so that only hot carriers can interact with it (Fig. 12) [102]. However, as the resonant scattering takes place in the latter situation whereas it is not present in semiconductors with extremely narrow levels, the scattering can now lead to the appearance of an S-shaped portion of the $I-U$ curve following the N-shaped part (Fig. 13) [102] and is caused by the same overheating mechanism that takes place for the short-living resonances. But as the S-part can appear only for certain electron scattering conditions, in many cases the effect of quasi-localized levels on the hot carrier transport will result in N-type NDC independently of the mechanism of the centre–band carrier transitions (elastic or inelastic) if only the inequality $\tau \geqq \tau_p$ is satisfied.

Now one can see a possible reason why resonant scattering of carriers was observed in $Pb_{1-x}Sn_xTe$(Tl), but not in $Pb_{1-x}Sn_xTe$ doped with In. The Tl resonant state is wide ($\gamma \approx 2$ meV) [107] and hence relatively short-living ($\tau \approx 10^{-13}$ s), whereas the In level is extremely narrow and long-living ($\gamma \leqq 0.01$ meV) [9]. So on the one hand, only a very small

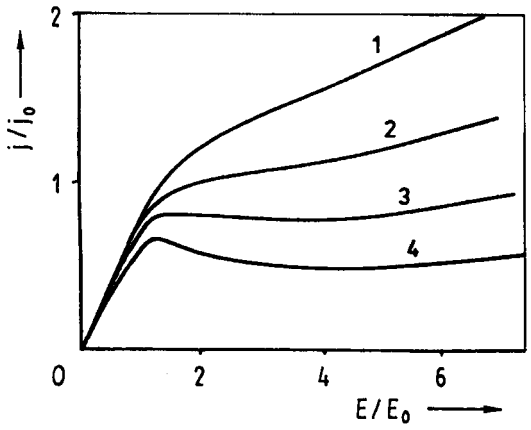

Fig. 12. The calculated $I-U$ curves in case of resonant scattering and scattering by DA phonons. The concentration of resonant centres increases from (1) to (4) [102]

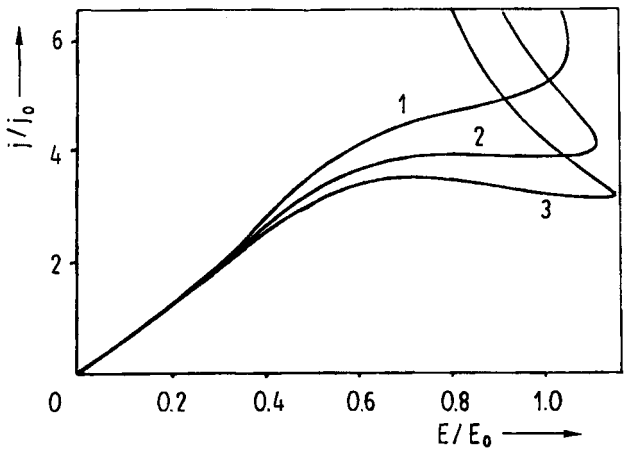

Fig. 13. The calculated $I-U$ curves in case that momentum relaxation of carriers is due to resonant and charged impurity scattering and their energy relaxation is due to DA scattering. The concentration of the resonant centres increases from (1) to (3) [102]

fraction of electrons can interact with the In state even at low temperatures and, on the other hand, for the long-living level inelastic collisions may interrupt the resonant scattering process thus preventing its manifestation. The decrease of temperature reduces the rate of inelastic processes as well as the carrier distribution width, so one can suppose that at temperatures low enough the resonant scattering should become observable for the In impurity, too. However, the observation of resonant scattering is possible only in the time interval much greater than τ, when the resonant scattering process has enough time to complete [108], and as the lifetime of the In level exceeds several days at helium temperatures, the observation of this kind of scattering seems to be very complicated.

6.3 Hot electron phenomena in $Pb_{1-x}Sn_xTe(In)$; experiment

We will stop here the account of the theoretical concepts and will turn to the results of the experiments carried out on $Pb_{1-x}Sn_xTe$ alloys in high electric fields. In this kind of experiments short field pulses are usually used to avoid sample heating [88]. To have a reference point, we will first describe the hot electron experiments in "ordinary" $Pb_{1-x}Sn_xTe$, and then turn to the situation in $Pb_{1-x}Sn_xTe$(In) and $Pb_{1-x}Sn_xTe$(Ga).

In n-$Pb_{1-x}Sn_xTe$ solid solutions not containing In, Ga, Tl, and similar impurities the measured $I-U$ curves at the temperatures of liquid nitrogen and liquid helium have a long sublinear part (up to electric fields of order of several tens kV/cm) and in higher fields there is an NDC region that can be either of S- or N-type [92, 96, 109]. The type of NDC may change when the alloy composition is varied as shown in Fig. 14 [92]. In the NDC region additional non-equilibrium carriers were observed as well as high field domains and current instabilities [96, 97, 110]. The appearance of the domains and instabilities was explained in [92, 109, 111] under the assumption that there existed an additional heavy extremum in the conduction band (so-called W extremum) so that the Gunn effect could take place. The threshold field for the onset of a domain instability depends upon the alloy composition and is equal to ≈ 1.5 kV/cm in n-PbTe and ≈ 0.5 kV/cm in n-$Pb_{0.8}Sn_{0.2}Te$ [109]. This dependence was explained in [109] by the decrease of the W–L energy separation Δ_{cw} when the SnTe content in the alloy was increased. Using the obtained experimental data, the Δ_{cw}

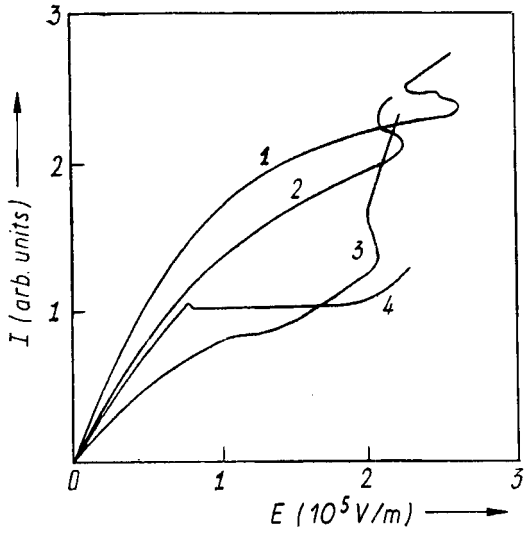

Fig. 14. $I-U$ curves of n-$Pb_{1-x}Sn_xTe$ specimens at 77 K for different x-values. (1) $x = 0$, (2) 0.06, (3) 0.12, (4) 0.18 [92]

dependence on x was established as

$$\Delta_{cw} = 0.17 - 0.54x + 6\times10^{-5}T + 2\times10^{-6}P,$$

where T is the temperature in K, P the hydrostatic pressure in 10^8 Pa. However, no independent evidence supporting the existence of the W minimum is available up to now. The alloy composition dependence of Δ_{cw} [109] gives the value of $\Delta_{cw} = 3.5$ meV for the popular $Pb_{0.75}Sn_{0.25}Te$ alloy, so that the W extremum would be rather close to the edge of the conductivion band, but there was no report on its effect upon any phenomenon. It is worth noting also that for compositions close to PbTe the calculated Δ_{cw} value is of order of E_g, so that the interband breakdown could also take place in the field region of the domain instability bringing about the increase of carrier concentration and of the current [96, 112]. The kinetics is quite complicated in this regime and further investigations are necessary to make clear the role of impact ionization and higher bands in the hot electron phenomena in $Pb_{1-x}Sn_xTe$ and their influence on the shape of $I-U$ curves and the parameters of current instabilities.

In the experiments [92, 109, 111] the doping level of the "ordinary" impurities did not influence the threshold field value of the instabilities, and it supported the assumption that the instability mechanism was the Gunn effect. On the contrary, the addition of In in $Pb_{1-x}Sn_xTe$ had a significant effect on the domain parameters and the $I-U$ curves. In [11] the high field non-equilibrium electron properties were investigated in n- and p-type $Pb_{1-x}Sn_xTe$(In) with $x = 0.2$ to 0.3 and In content ≈ 0.5 at%. The In concentration was large enough to pin the Fermi energy in the band, so that the samples were in the so-called metal state. The measurements were carried out at low temperatures 4.2 to 40 K under hydrostatic pressure up to 10^9 Pa using current pulses ≈ 8 μs long. In n-$Pb_{1-x}Sn_xTe$(In) the non-linear $I-U$ curves, N-type NDC, and the domain formation were observed in electric fields lower than 10 V/cm that is two orders of magnitude less than in undoped material. The $I-U$ curves had a large hysteresis so that the N-shaped part was observed only when the field was increased (Fig. 15). The portion of the curve corresponding to the decrease of the field lay much lower so that the sample conductivity decreased noticeably after the field pulse. Then the conductivity relaxed slowly to its high initial value during about ten minutes. In p-type material the field corresponding to the N-part was somewhat higher (about 20 to 40 V/cm) and the hysteresis was not observed.

The high field domains in the alloys doped with In have properties different from those of the ordinary Gunn domains. Their velocity depends sharply upon the applied field, so that it is of the order of 10^2 cm/s at the instability threshold and increases up to $\approx 10^6$ cm/s

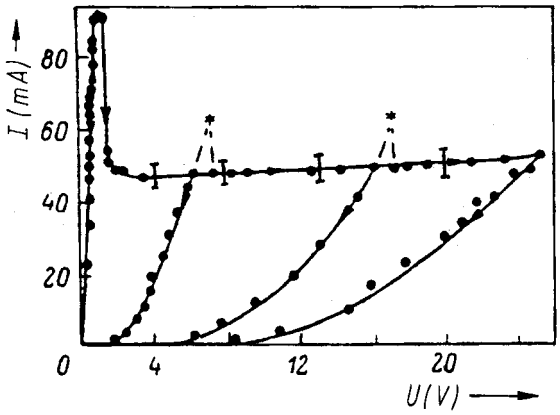

Fig. 15. I–U curves of n-$Pb_{1-x}Sn_xTe$(In), $x = 0.21$ (metallic state). The length of the sample was 2.5 mm [11]

at the field of 40 V/cm, the maximum field value used in [11]. The domain does not disappear when the field is turned off and remains stable during several ten minutes at 4.2 K. Hall effect measurements show that the carrier concentration in the domain is strongly reduced as compared to its initial value whereas the mobility remains unchanged. The most natural assumption is that the domain formation in the doped alloys is connected with the capture of hot electrons by the In level. The situation is similar to the concentration instability in a semiconductor doped with negatively charged impurities [105], and it is one more evidence for the existence of a barrier that complicates the electron transitions from the band to the centres and vice versa.

The attempt to investigate the graduate change of the domain properties and the instability mechanism due to the change of In content in the material was made in [111]. The In concentration in the samples was 0.03, 0.3, and 0.5 at%, the alloy composition $x \approx 0.2$, and the temperature 4.2 K $\leqq T \leqq$ 77 K. The domain instability was observed in all the samples and the threshold field was in the range 300 to 500 V/cm, i.e. it was as high as in undoped material. However, the domain velocity v at temperatures less than 50 K decreased according to an activation law so that $v(5\text{ K})/v(77\text{ K}) \approx 0.2$. The increase of In concentration from 0.03 to 0.5 at% led also to a decrease of velocity. The domain lifetime after switching off the field also increased according to an activation law when the temperature was decreased and became sometimes as large as 10 min.

The data obtained in [11] and [111] showed that the In impurity states influenced strongly the domain instability in $Pb_{1-x}Sn_xTe$. Some contradiction between the results of the two investigations cited can be caused by the use of current pulses of different lengths, 8 μs in [11] and 10 ns in [111]. It seems reasonable that the slow process of electron transitions between band and impurity states can manifest itself more prominently for longer pulses.

The phenomena described above were observed when the In level lies in a band (metallic state). But in the composition range near $x = 0.25$ the level is situated within the gap and the material becomes semi-insulating because the Fermi energy is pinned to the level. Static I–U curves of the semi-insulating material were investigated in [10]. The authors of [10] applied a dc electric field to their samples, not field pulses. In the dark the initial low current part of the I–U curve was non-linear and could be described by $I \sim U^2$. The physical mechanism leading to the formation of this part has not been unambiguously established.

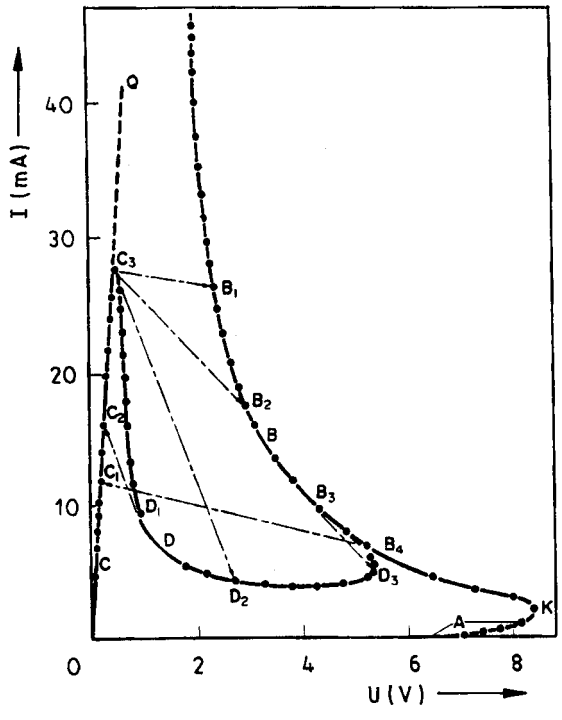

Fig. 16. Dc $I-U$ curves of $Pb_{1-x}Sn_xTe(In)$, $x = 0.25$ (dielectric state) in the dark (A, B) and under infrared illumination (C, D, B). The length of the sample was 2.9 mm [10]

Probably it was caused by carrier injection from the contacts into the semi-insulating sample. However, in [121] the formation of this part of the $I-U$ curve was attributed to a ferroelectric phase transition [122, 123].

At higher voltages the $I-U$ curves have an S-shaped part associated in [10] with the electrothermal breakdown. (The direct evidence for this interpretation was later found in [113].) Under IR-illumination of samples with ionized In impurities the additional N-shaped part appeared in weaker field (Fig. 16). It was explained by a fast decrease of the non-equilibrium carrier lifetime as their temperature increased due to the exponential increase of the In trap cross-section. The cross-section increase was connected with the existence of a barrier for band–In impurity transitions. The field heating of carriers led to an increase of the capture rate and hence to an electron concentration decrease resulting in the N-type NDC. These results were later reproduced in [114] using In-doped thin $Pb_{1-x}Sn_xTe$ films with $x = 0.22$.

The highly conducting non-equilibrium state that appeared due to the breakdown was shown in [115] to be practically stable in space and time at helium temperatures so that no diffusion or relaxation of excited carriers could be observed during several minutes (the duration of the experiment) if only a part of a sample was switched to this state. The local switching could be done either by illumination of the sample with a local IR-light spot or by application of a voltage to a part of the sample using a grid of contacts. The increase of the conductivity after excitation was by about four orders of magnitude. The initial dielectric state could be restored only by heating the sample to temperatures exceeding 20 K or by application of microwave pulses (see Section 8). These experiments have demonstrated that the long-living non-equilibrium electrons appear in the band due to the ionization of impurities and hence they could not diffuse deeply into the unexcited part of the sample because of the Coulomb attraction to their native impurity ions. The extremely slow relaxation rate of the non-equilibrium state showed again the existence of a barrier slowing down the impurity–band carrier exchange.

6.4 Properties of PbTe(Ga) in high electric field

Let us turn now to the high field properties of PbTe(Ga) [116]. The samples investigated were semi-insulators at the temperature of liquid helium. At 4.2 K they could be of either

n- or p-type conductivity and the concentration of carriers was as low as 10^{10} to 10^{12} cm^{-3}. The carrier mobility was 10^3 to 10^5 cm^2/Vs. Unlike in [10], where semi-insulating $Pb_{1-x}Sn_xTe(In)$ was investigated in dc fields, short pulses of electric field (0.03 to 40) μs were used here to avoid sample heating. It was found that in fields of 100 to 400 V/cm the dependence of I on U obeys the law $\ln I \sim E^{1/\gamma}$, $\gamma = 1.9$ to 2, which can be explained by the Poole-Frenkel mechanism [117] or by non-ohmic hopping conduction [118]. At higher fields ≈300 to 1000 V/cm impurity breakdown was observed (some specific features of the process showed that it was impurity breakdown indeed and not interband breakdown that was observed in undoped PbTe [96] in the same field region). The breakdown led to a conductivity increase by a factor of 10^7 to 10^8 at 4.2 K. The lifetime of the non-equilibrium carriers appearing due to the breakdown was very long, of the order of 10^5 s. When the temperature was increased the lifetime decreased and became less than 10^{-2} s at 77 K.

It is worth noting that the highly conducting state that appears in PbTe(Ga) as a result of the breakdown is not spatially uniform. It was established in [116] using a grid of contacts. The structure of the highly conductive part of the sample changes from one experiment to another. However, the simple method used in [116] did not allow to investigate the structure of this state in detail.

So one can conclude that the physical phenomena in semi-insulating PbTe(Ga) are similar to those observed in In-doped material, and they can also be connected with the long-living defect states introduced by doping.

6.5 Tunneling spectroscopy of doped lead–tin telluride

It was shown above that the quasi-localized levels influence significantly the hot electron phenomena in MLTA. However, it is rather complicated to get information on the parameters of the level using hot electron data, first, because the hot electron transport is a complex phenomenon that is influenced by a large number of different factors and many of them need investigation in their turn, and second, because the distribution function of hot carriers is wide in energy and so the current is not sensitive to fine details of the level structure.

On the contrary, tunneling spectroscopy uses non-equilibrium carriers with well-defined energy, so it is a very convenient method to investigate the structure of the density of states and, in particular, to define position and shape of the quasi-localized levels.

This technique was applied to PbTe doped with Tl or In by Kaidanov and coworkers [12, 107, 124, 125]. The tunneling structures $Pb/Al_2O_3/PbTe$ or Pb/ZnS/PbTe were prepared on bulk crystals of doped or undoped PbTe. Application of the quantizing magnetic field to the structure and observation of the quantum oscillations of the tunneling current were used to establish the connection between the bias applied to the structure and the energy of the injected electrons with respect to the band edges of PbTe. In both undoped and doped material independently of the kind of impurities a kink on the I–U curves was observed in the valence band at the energy $\varepsilon_{v\,max} - \varepsilon = 0.235$ eV. The kink was attributed to the edge of the second valence band (Σ extremum).

In the structures with PbTe (0.2 at% Tl) an additional peculiarity on the I–U curve was found [107], i.e., a peak at $\varepsilon_{v\,max} - \varepsilon = 0.222$ eV. The peak was situated very close to the position of the Tl level determined from mobility measurements [8], so the peak was associated with quasi-localized Tl states. The shape of the peak is close to a Lorentzian (a Gaussian does not fit to the data) so that the corresponding density of quasi-local states

can be expressed as

$$\varrho_i(\varepsilon) = \text{const}/[(\varepsilon - \varepsilon_i)^2 + \gamma^2]$$

with $\gamma = 2 \times 10^{-3}$ eV [107]. The amplitude of the peak is about 10% of the background so that ϱ_i is much less than the density of states in the valence (light hole) band at the same energy. The observed Lorentzian shape of the impurity level supports the assumption that the main reason of the level broadening is the hybridization of impurity and band states. Using this γ-value, the lifetime of the quasi-local state can be estimated as $\tau = h/\gamma \approx 10^{-13}$ s that is much less than the momentum relaxation time that corresponds to a carrier mobility of the order of 10^4 to 10^5 cm^2/Vs common for PbTe. Hence the resonant state of Tl is relatively short-living.

The situation is quite different in case of In-doped PbTe [12]. Instead of the peak induced by the quasi-localized level the $I-U$ curve now shows a hysteresis and a series of oscillations. The interpretation of these peculiarities is rather complicated and we will not reproduce it here, referring the reader to the original paper [12]. It is worth noting that it was possible [12] to explain the results on the basis of the model [9, 10] of In-induced centres (see Section 5). As the model included barriers for the transitions, it could lead to the extremely slow carrier exchange rate between the centre and the band, which was the main reason for the hysteresis phenomena. So the tunneling experiments gave a new evidence for the long-living In-induced state. However, it was impossible to extract any information on the width of the quasi-local level from these experiments.

7. Optical and Photoelectric Properties of $Pb_{1-x}Sn_xTe$(In) and PbTe(Ga)

7.1 Optical absorption in the group III-doped lead telluride-based alloys

Generally, optical measurements are one of the most reliable tools for the investigation of impurities in semiconductors. One can get from optical absorption measurements the energy position of an impurity level and its shift with changing temperature or any other external factor.

This kind of experiments has been performed for the MLTA doped with different group III impurities: B [126], Al [127], In [128], Ga [30], Tl [129]. The general result of these experiments is the following. For all the group III impurities in PbTe only resonant levels have been detected. The level position depends on the atomic number of the impurity: the heavier the impurity atom, the lower is the energy of the respective level. Whereas for B, Al, Ga the levels are rather high in the conduction band, for In they are near its bottom and for Tl in the valence band ($T = 300$ K). However, this conclusion is not very strict. For example, it is known (see Section 2) that there exist several saturation regions in the dependence n, $p(N_{Ga})$. Every region is believed to correspond to the formation of a local or resonant level. Apparently the data reported in [30] correspond to the resonant level highest in energy.

Most of the optical absorption experiments deal with indium-doped $Pb_{1-x}Sn_xTe$. It has been shown in [128, 130 to 132] that there exists some additional absorption at energies below the fundamental one both when the level is resonant ($x < 0.22$) and when it is local ($0.22 < x < 0.28$). This additional absorption was attributed to conduction band–impurity or impurity–conduction band transitions. The spectra have been taken at temperatures $T > 77$ K, so no singularities due to the persistent photoconductivity could be detected.

In a later paper [65] the measurements have been performed down to helium temperatures. These data show that the structure of the impurity states is rather complex. Indeed, it has been observed that the optical absorption in $Pb_{1-x}Sn_xTe(In)$ decreases in time. This effect is believed to be due to the fact that part of the absorption is due to the optical transitions between ground two-electron and metastable one-electron quasi-local states. The ground and metastable local states and the extended states are separated by barriers in the configuration coordinate space, so they are long-living (see Section 5). When most of the metastable states become populated, the sample transparency increases. The concentration of metastable states has been estimated from these measurements. This value turns out to be much lower ($\approx 10^{17}$ cm^{-3}) than the total indium concentration in the sample ($\approx 10^{19}$ cm^{-3}). The authors of [65] come to the conclusion that the centres may be impurity–defect complexes.

Very interesting results on the sub-bandgap optical absorption in $Pb_{0.78}Sn_{0.22}Te(In)$ are presented in [133]. A sharp absorption peak at $\omega_{loc} = 160$ cm^{-1} was observed. This peak was attributed to the local mode of In in the $Pb_{1-x}Sn_xTe$ lattice.

7.2 Photoconductivity spectra of the indium-doped lead telluride-based alloys

Infrared illumination of the In-doped lead telluride-based alloys leads to the appearance of a persistent photoconductivity effect at low temperatures $T < 20$ K. The effect originates from the existence of a barrier between the local and extended electron states of the system in the configuration coordinate space (see Section 5). Generally, it is clear that the red cut-off wavelength of the photoresponse should be very long provided the characteristic energies of the electron spectrum are small. However, as long as deep impurity centres are concerned, the optical activation energy may exceed significantly the thermal one. Measurements of the photoconductivity spectra may provide important information on the structure of impurity states.

The experimental solution of the problem is not straightforward. Indeed, in an ordinary spectroscopic equipment there exists a long-wavelength room temperature background radiation. The photoexcited free carriers accumulate in the bands, therefore this background radiation may transfer the sample to a highly non-equilibrium state already during the cooling-down process.

This was understood from the very beginning, so there were not too many attempts to investigate the photoresponse spectrum. An unusual indirect technique has been proposed in one of the first papers dealing with the persistent photoconductivity effect in $Pb_{1-x}Sn_xTe(In)$ [134]. A sample with $x = 0.25$ (dielectric state) has been cooled to $T = 4.2$ K in a light-tight cell, so initially there were no excited electrons in the conduction band. A carbon resistor has been used as an internal IR-radiation source. Assuming the radiation to be black-body-like and comparing the rates of the conductivity rise for different black-body temperatures, one can deduce the red cut-off energy. It has been shown that the optical activation energy equals the thermal one within the experimental accuracy of 20%. This result is not usual for a deep impurity centre which is separated by a barrier from extended states. However, it can be understood if one takes into account that the electron activation energy is close to the LO-phonon energy, so the Frank-Condon principle may be violated.

The estimates done in [134] are not very accurate, and it is clear that direct spectral measurements are much more preferable. These low temperature ($T = 4.2$ K) measurements have been performed in [135 to 140] with the ordinary spectroscopic equipment. It means

that a high concentration of electrons excited by the background radiation existed initially in the samples. The composition of alloys in all experiments has been chosen $x > 0.22$ in order to provide the lowest possible "dark" free electron concentration. In all experiments [135 to 140] high photoconductivity at sub-bandgap energy has been observed. No pronounced structure of the photoresponse spectrum has been detected in [137 to 140]. On the contrary, it has been reported in [135, 136] that the spectral sub-bandgap tail of the photoresponse consists of several bands. One of them is of Gaussian shape, that is not usual for impurity photoconductivity. This band is associated in [135, 136] with transitions between the ground and metastable local states. The question arises, how the transitions between two local states can contribute to photoconductivity. The explanation presented in [135, 136] is as follows. Photoexcitation of the transitions leads to an excess population of the metastable impurity states. The latter may lie on the background of the conduction band and may be separated by only a small barrier from the extended states. Thus thermal or background optical excitation would lead to electron delocalization. In fact, [135, 136] belong to the first papers giving some indications on effects due to the existence of metastable impurity states in $Pb_{1-x}Sn_xTe$(In).

One should pay special attention to a series of papers by Zasavitskii et al. [64, 141, 142], where the photoconductivity spectra of $Pb_{1-x}Sn_xTe$(In) have been investigated in the presence of either a controlled flux or complete screening of background radiation. Far-infrared lasers have been used as radiation sources of definite wavelength. The photoconductivity spectra measured in [64, 141, 142] seem to be most "clean" from the experimental point of view. The most interesting effect observed in these experiments is a negative photoconductivity. The composition of the samples was $x = 0.23$, so the dielectric state of the system was realized. When the sample at $T = 4.2$ K is illuminated by both long-wavelength background radiation and short-wavelength laser pulses, a strong increment of the sample resistivity is detected after the pulse end (negative photoconductivity). If the energy of the short-wavelength laser light E_{sh} is lower than some threshold value, the negative photoconductivity signal coexists with the positive one. If the energy E_{sh} is lowered even more, only positive photoconductivity is observed. The results in [64, 141, 142] have been interpreted in the framework of the model taking into account the existence of a metastable one-electron quasi-local state separated by barriers in the configuration coordinate space from both extended and ground two-electron local states. Considering different kinds of optical transitions between those states the authors of [64, 141, 142] came to the conclusion that the coexistence of the negative and positive photoconductivity signals may be provided only if there exist metastable one-electron local states. It is assumed that the direct two-electron transitions from the local ground state E_2 to the extended one E_0 are of negligible probability, transitions of this kind can occur only via the metastable one-electron local state E_1. Rising the light quantum energy E_{sh} above the threshold value results in the excitation of an electron from the valence band to the E_1 state. A free hole recombines with the photoexcited free electron during the time $\approx 10^{-7}$ s. This process gives rise to the negative photoconductivity signal. A similar effect has been observed in experiments of another group [143].

Taking into account the temperature dependence of negative and positive photosignals the parameters of local states in $Pb_{1-x}Sn_xTe$(In) have been calculated in [65] (see Section 5). However, there are some quantitative discrepancies in the results of calculations [141]. It means that the simple model can only be applied as a qualitative scheme. However, it fails if one tries to make quantitative estimates. From this point of view the attempts to calculate

the dependence of the parameters of the local states on the alloy composition [65] seem to be of not too much value.

Moreover, the effect of negative photoconductivity has also been detected in experiments of another group [135, 136], but in the latter case the negative photoconductivity signal was observed when the sample was illuminated by long-wavelength radiation in addition to the background one. So one can see that the information concerning this effect is rather contradictory.

7.3 Peculiarities of the photoconductivity spectra of PbTe(Ga)

The persistent photoconductivity effect is observed in lead telluride doped with another group III impurity, gallium. The effect has been detected in samples being in the dielectric state. There is a number of papers where the photoresponse spectra of PbTe(Ga) have been measured. Usually the measurements have been performed at temperatures $T \geqq 77$ K, where the lifetimes of photoexcited free carriers are not so high ($\tau < 10^{-2}$ s), and the ordinary spectroscopic techniques are applicable. The common result of these experiments is the absence of a pronounced impurity photoconductivity. In some papers it is not detected at all [144, 145], in others only a slight photoresponse with sub-bandgap energies is observed [62, 146 to 148]. Anyway, this is in contrast to the case of In-doped lead–tin tellurides, where the amplitude of the impurity photoconductivity was by the order of magnitude comparable with the band-to-band photoresponse [135, 136]. This is rather surprising, because the existence of an impurity level with high density of states is well established from galvanomagnetic measurements [31, 62, 145, 148]. An explanation of this effect has been proposed in [144]. Direct optical impurity–conduction band transitions in the configuration coordinate space may have an energy higher than the bandgap. The phonon energies are much lower than the energies of the electronic spectrum, so the Frank-Condon principle is not violated, in contrast to the case of $Pb_{1-x}Sn_xTe$(In). Thus the impurity photoconductivity band lies on the background of the fundamental absorption and is not seen.

Recently Belogorokhov et al. [144] have observed a high selective photoresponse in the far-infrared $\omega_p = 130\ cm^{-1}$ in the liquid nitrogen temperature region $T \approx$ (60 to 65) K in the PbTe(Ga)-based alloys with the Fermi level pinned within the gap. The spectra have been taken using a Fourier-transform spectrometer, so the sample has been illuminated by radiation with a broad excitation spectrum. The energy value corresponding to ω_p is much lower than any characteristic energy of the electronic spectrum of PbTe and impurity activation energy in PbTe(Ga). At the same time ω_p is close to the energy of the LO-phonon in PbTe $\omega_{LO} = 110\ cm^{-1}$ [149]. The results in [144] have been interpreted in terms of phonon- or local mode-assisted transitions from the metastable impurity level to the conduction band. It is believed that the short-wavelength radiation excites electrons to the metastable local state that may lie on the background of the conduction band, or at least close to its edge. The radiation with $\omega = \omega_p$ interacts with the lattice, and electrons are ejected from the metastable state to the conduction band giving rise to the photoresponse. This result is the first one that is believed to be due to the existence of metastable impurity states in PbTe(Ga) with pinned Fermi level.

7.4 Infrared reflection spectra of Indium-doped lead–tin tellurides

Most of the papers dealing with the reflection spectra of $Pb_{1-x}Sn_xTe$(In) [150 to 153] do not provide fundamentally new information with respect to the galvanomagnetic measure-

ments: it was shown that the plasma frequency increases at low temperatures, that is apparently due to the persistent photoconductivity effect. The most interesting result in this range of papers is reported in [151]: it was observed that the hydrostatic pressure practically does not influence the photoresponse. This is in contrast to the result obtained in [51], where it was shown that the application of external pressure speeds up the local level–conduction band transitions in a magnetic field.

Romcevic et al. [154] have observed an additional structure in the reflection spectra of $Pb_{0.75}Sn_{0.25}Te(In)$ at temperatures below $T_c \approx 20$ K, the temperature of appearance of the persistent photoconductivity effect. An additional oscillator has been introduced into the usual plasmon–phonon dispersion relation in order to fit the experimental spectra at $T < 20$ K. The oscillator strength decreases to zero at $T = 20$ K with increasing temperature. Its frequency slightly depends on temperature, at $T = 4.2$ K it is a little bit less than the impurity activation energy. The oscillator has been attributed to the optical transitions between ground and metastable impurity states. Indeed the data presented in [155] allow to conclude that the metastable impurity level lies just below the conduction band bottom in the alloy with $x = 0.25$. This corresponds to the measured oscillator frequency. The disappearance of the oscillator at $T = 20$ K is believed to be due to the reconstruction of the $Pb_{0.75}Sn_{0.25}Te(In)$ configuration coordinate diagram with changing temperature: the barrier separating metastable and ground impurity states disappears, and the lifetime of the metastable state becomes very small at $T > 20$ K (Fig. 17). However, no calculations that could support this interpretation have been presented in [154].

A similar effect has been observed in PbTe(Ga) with the Fermi level pinned within the gap [156]. In contrast to the case of In-doped samples an additional oscillator is present in the reflection spectra even at $T > T_c = 80$ K, where the persistent photoconductivity disappears in PbTe(Ga). However, the oscillator strength sharply rises at $T < T_c$. So the origin of this additional oscillator is assumed to be the same as in the case of $Pb_{1-x}Sn_xTe(In)$. It should be noted that [156] together with [144] are the only papers we know that contain some experimental evidence for the existence of metastable impurity states in PbTe(Ga).

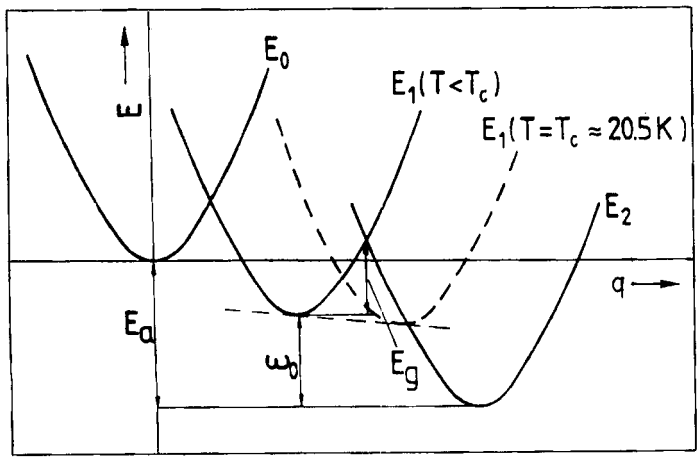

Fig. 17. Reconstruction of the configuration coordinate diagram of the centre in $Pb_{0.75}Sn_{0.25}Te(In)$ when the temperature is varied [155]. At $T = T_c$ the barrier separating metastable (E_1) and ground (E_2) states disappears

Analyzing the results obtained in [154, 156], it sems to be likely that the appearance of a persistent photoconductivity effect corresponds to the formation of a barrier in the configuration coordinate space between ground and metastable impurity states. This hypothesis explains also the non-exponential photoconductivity relaxation at $T < 20$ K [64], the dependence of the photoconductivity relaxation rate on the level of initial photoexcitation [53], and some other effects.

On the other hand, the effects observed in [154, 156] may have a different explanation. For example, an additional structure has been observed in the reflection spectra of undoped $Pb_{0.8}Sn_{0.2}Te$ at $T = (200$ to $400)$ K, $\omega \approx 100\ cm^{-1}$ [157]. This structure was attributed to the electron transitions between local and extended states. One cannot exclude that this structure is due to a local impurity mode, though there exist arguments against this statement [154].

Spectral measurements of infrared absorption, reflectivity, and photoconductivity reveal a complex structure of impurity states in the In- and Ga-doped lead telluride-based alloys. Part of the data give some evidence for the existence of metastable impurity states that play a significant role in some non-equilibrium effects. However, the results of experiments do not give clear information on the parameters of these states. Even their energy position and the shape of the density of states are not well established.

8. Galvanomagnetic and Photoelectric Phenomena under Combined Action of External Factors

8.1 Electric and magnetic fields

External factors, such as magnetic and electric fields, pressure, infrared illumination, strongly affect the properties of the group III-doped lead telluride-based alloys. This is a consequence of the fact that the characteristic electronic energies are rather small and may be considerably modified by varying the above-mentioned parameters. The combined action of external factors leads to the appearance of new effects. These effects are especially pronounced when the material is in the dielectric state, i.e. when there are practically no free carriers at low temperatures. Indeed, in this case a small modification of the respective position of energy levels (e.g., impurity level and conduction band bottom) results in strong changes of the free carrier concentration. This is the reason why in most papers investigating this kind of effects the range of materials is restricted to In-doped lead–tin tellurides, where the dielectric state may be easily realized.

The unusual galvanomagnetic properties of $Pb_{1-x}Sn_xTe$(In) under the combined action of electric and magnetic fields are the first example in this series of effects.

As was discussed in Section 6.3, the current–voltage characteristics (CVC) of $Pb_{1-x}Sn_x$ · Te(In) with the Fermi level pinned within the gap (dielectric state) are S-shaped at low temperatures. The rising branch of CVC is superlinear ($I \sim U^2$) at $T < 8$ K. The form of the rising branch of CVC at low temperatures is probably determined by the monopolar injection of electrons from the contacts. The actual value of the injection current at a fixed voltage, however, is much lower than it would be expected for an ideal trap-free insulator. This means that the trapping of electrons plays an important role in the processes involved.

Some information on the properties of the trapping centres has been obtained in the experiments with magnetic fields [155]. The $Pb_{0.75}Sn_{0.25}Te$(In) sample with the Fermi level pinned at ≈ 20 meV below the conduction band bottom has been cooled down to $T = 4.2$ K.

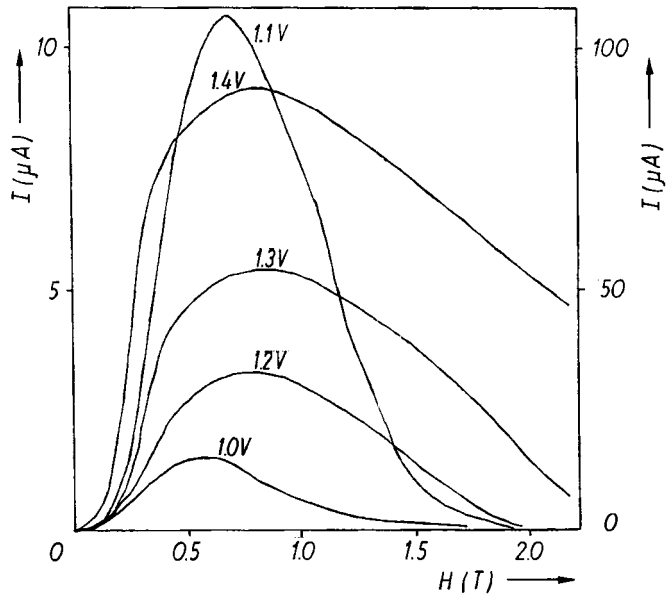

Fig. 18. Dependence of the sample current on the applied magnetic field for $Pb_{0.75}Sn_{0.25}Te(In)$ at $T = 4.2$ K [156]. The figure near the curve is the voltage applied to the sample

Application of a rather low magnetic field $H \approx 0.5$ T leads to drastic changes in the rising branch of CVC. For every fixed voltage the respective value of current increases. By analogy with the ohmic CVCs one can see that negative magnetoresistance is observed. The effect has been detected by both four-probe and two-probe techniques. In the latter case the sample current has been measured as a function of the magnetic field applied. The results are shown in Fig. 18. The sample current I has a pronounced peak at $H_{max} \approx 0.5$ T. The peak amplitude increases quickly when the applied voltage is raised. It is interesting to note that in some cases the negative magnetoresistance amplitude is $I(H_{max})/I(H = 0) > 10^6$.

The effect has been explained in [155] by the motion of a metastable impurity level in magnetic field. Indeed if this level lies just below the conduction band bottom and is separated by a relatively small barrier $W \approx 1$ meV from the conduction band [64, 142], it may be an effective trap for injected electrons. If the level moves upwards in energy in magnetic field then its depopulation will lead to an increase of the free electron concentration, the latter will approach its "trap-free" value, and the sample conductivity will rise. In magnetic field $H = H_{max}$ the conductivity starts to diminish probably due to a mobility decrease.

This consideration has been supported in [158] by Hall effect measurements. It has been shown that the Hall coefficient drops significantly in a magnetic field $H \approx 0.5$ T. The measurements in [158] have been performed for slightly illuminated $Pb_{0.75}Sn_{0.25}Te(In)$. This has been done in order to provide some ohmic conductivity of the sample, because otherwise correct Hall measurements were impossible. The effect of ejection of electrons from the traps in magnetic field was clearly seen even on the background of the photogenerated free electrons.

8.2 Strong magnetic field and infrared illumination

In the experiments described in [158 to 160] the external infrared illumination has been used as one more factor affecting the respective position of the quasi-Fermi level and the energy bands in $Pb_{1-x}Sn_xTe(In)$. In fact, it allows to move smoothly the quasi-Fermi level, because the photogenerated free electrons are long-living. We have seen that for low free electron concentrations application of a magnetic field $H \approx 0.5$ T led to the delocalization of electrons. The more surprising is the fact that for higher magnetic fields $H > 5$ T, on the contrary, the localization of free photogenerated electrons has been observed [158 to 160]. In these experiments the magnetoresistance of $Pb_{1-x}Sn_xTe(In)$ samples has been measured in pulsed magnetic fields H up to 40 T. The high field installation allows to make the pulse top flat, of ≈ 0.5 s length. It turns out that the sample resistance increases with time exponentially during the flat top of the pulse. The characteristic time depends exponentially on the magnetic field and linearly on the temperature,

$$\tau = \tau_0 \left(1 - \frac{T}{T_0}\right) \exp\left(\frac{H}{H_0}\right),$$

where $H_0 \approx 4.5$ T does not depend neither on the sample temperature nor on the concentration of photoexcited electrons (quasi-Fermi level position), nor even on the amount of indium in the material. The value of $T_0 \approx$ (4 to 6) K decreases with increasing free carrier concentration, and the effect is not observed for $T > T_0$. The value of $\tau_0 \approx 10^{-2}$ s by the order of magnitude corresponds to the characteristic time of the initial fast drop of the persistent photoconductivity after the illumination is switched off [53]. The latter process is associated in some papers (see, e.g., [161]) with the recombination at the metastable impurity level.

The authors of [158 to 160] have analyzed different possible mechanisms of the effect : influence of energy band modulation, magnetic freeze-out on shallow impurities, localization on deep impurity levels. It has been shown that none of them can explain unambiguously the effect in all details. It seems to be most likely that the effect is due to the localization of non-equilibrium electrons at the metastable impurity level in a high magnetic field. However, the arguments given in support of this statement – absence of a dependence of H_0 on any external factor, proximity of τ_0 to the characteristic time of the initial photoconductivity drop – are not quite convincing. Moreover, it has been shown in [158] that when the free electron concentration is high enough, so that T_0 becomes less than T, one observes, instead, the delocalization of electrons. So if all three effects – delocalization in low magnetic field resulting in giant negative magnetoresistance [155], localization in high fields at relatively low concentration of photoexcited electrons [158 to 160], and delocalization at higher electron concentration [158] – are due to the peculiarities of the same metastable impurity level, the latter must have a very unusual structure.

8.3 Electric or microwave fields and infrared illumination

One can see that the combined action of external factors reveals some very unusual properties of the impurity states in $Pb_{1-x}Sn_xTe(In)$. Another example of this kind is the combination of infrared illumination with high electric or microwave fields.

The interest in this problem is strongly stimulated by applied aspects. Indeed, integration of the light flux in photodetectors is a very efficient way to increase the signal-to-noise

ratio of a device. In $Pb_{1-x}Sn_xTe(In)$ the incident light flux is internally integrated due to the persistent photoconductivity effect, and no external integrating circuits are needed. This makes it very attractive to use materials revealing persistent photoconductivity as infrared photodetectors. However, there arises the problem of erasing the information accumulated on the photodetector, i.e. the problem of fast quenching of the persistent photoconductivity.

One of the possible solutions of this problem is the application of strong electric field pulses to the sample contacts, as it has been shown already in the first paper dealing with the persistent photoconductivity effect in $Pb_{1-x}Sn_xTe(In)$ [52]. It has been demonstrated that this quenching is due to the electrothermal breakdown (see Section 6.3).

Electrothermal quenching has a characteristic time $\approx 10^{-2}$ s [10]. In many cases it is too slow for photodetector systems. Besides that, quenching produced in this way is complete only in the photomemory regime, i.e. if the light is off. If the photogeneration is permanent, and the electric field pulses are applied periodically to the sample contacts, the photoconductivity quenching will be unstable and not complete: the minimum value of conductivity after the pulse end is higher than in the initial "dark" state and changes from pulse to pulse. At last, periodical application of a high electric field to the sample contacts leads to an irreversible decrease of photoresponse and to its disappearance [162].

Another possibility for information erasing arises from the effect of high field domain instability which has been observed in $Pb_{1-x}Sn_xTe(In)$ alloys with the Fermi level pinned in the conduction band [11] and in the bandgap [163, 164]. The effect was discussed in detail in Sections 6.2 and 6.3. It should be noted that after the application of a short ($\approx 10^{-7}$ s) electric field pulse a domain is formed only in part of the sample. The size of the domain is usually much smaller than the sample length for a bulk crystal, so a dielectric-like state is formed only in part of the sample and is not very stable in size for different pulses.

This fast, purely electronic quenching has one disadvantage: the rather low resistance of the sample after quenching. This is due to the fact that the electric field applied to the sample is concentrated in a small region, so the injection current and the effective conductivity are rather high. One must enlarge the high-ohmic region in order to have a higher initial resistance.

Quenching of persistent photoconductivity by microwave pulses is free from this disadvantage [162, 165]. In this technique either the sample is installed in a microwave resonator or the microwave pulses are applied directly to the sample contacts. Experiments described in [162, 165] have been performed on samples with $x = 0.25$, in which the Fermi level is pinned within the gap. The microwave frequency was ≈ 400 MHz, the power P in a pulse up to 38 W, the pulse length ≈ 10 μs, and the sample was installed into a resonator. The sample resistance after the end of every microwave pulse did not differ from the initial "dark" resistance. Probably the quenching produced in this way is spatially homogeneous, and no high field domains are formed. Besides that, application of the short microwave pulses affects the photoresponse after the pulse end. It has been shown in [165] that if the persistent photoconductivity is quenched by microwave pulses of minimum length and amplitude necessary, the quantum efficiency of a photoresistor will increase up to $\approx 10^2$. An explanation of this effect of microwave stimulation of quantum efficiency has been proposed in [165]. Short microwave pulses result in the localization of photoexcited free electrons at the metastable local states, and not at the ground state. The metastable centres are believed to form clusters with strong internal interaction via the lattice deformation. So excitation of an electron from one of the cluster centre may lead to avalanche electron excitation from

other centres of this cluster. This gives rise to the increment of quantum efficiency. Longer or stronger microwave pulses localize the photoexcited electrons to the local ground state.

Apparently, the microwave quenching of persistent photoconductivity is due to the direct interaction of the microwave radiation with free electrons. Indeed, no lattice heating after the microwave pulse is observed [162]. One of the possible explanations of the microwave quenching effect is heating of the electron gas by the microwave pulse. In this case one would expect the quenching efficiency to be independent of the microwave frequency. However, there exists some evidence that this effect is resonant in frequency. The following experiment has been performed in [166]. A $Pb_{0.75}Sn_{0.25}Te(In)$ sample cooled down to 4.2 K has been included in two electric circuits. The first one has been used for the dc measurement of sample conductivity, the second one for microwave "pumping" of the sample. The microwave generator could sweep the frequency in the range (0 to 500) MHz. The pumping power has been ≈ 50 mW, which is much lower than the minimum power necessary for quenching, ≈ 900 mW. The dependence of the sample dc conductivity σ on the pumping frequency ω has been measured for different exposures to infrared illumination. In the initial "dark" state no conductivity in the whole frequency range is observed. As the infrared radiation exposure increases, a sharp peak at $\omega = 280$ MHz appears on the $\sigma(\omega)$ dependence on the background of a total conductivity rise. After the IR-radiation source is switched off, the conductivity slowly relaxes to the initial state, but the rate of this relaxation is much higher outside the peak frequency range than in the peak region. So the state can be reached that the sample conductivity is negligible for all frequencies except for the region of the peak. It is interesting to note that there is no zero-frequency dc conductivity. The position of this peak does not depend on the electric field applied (up to 50 V/cm), but depends strongly on magnetic field. For $H = 2$ T the peak shifts to $\omega = 50$ MHz. The sensitivity of the sample conductivity in the region of the peak to the action of IR-radiation is much higher than for the initial "dark" state of the sample. The authors of [166] did not give any clear interpretation of the effect, but indications exist that it is related with the effect of quantum efficiency stimulation. Indeed, both of them are observed in the same microwave frequency range. Besides that, it is obvious that in both cases the sample is transferred to a metastable high ohmic state that is much more sensitive to the action of IR-radiation than the initial dark state. So it seems to be likely that the relaxation of photoexcited free electrons to metastable impurity states is responsible for both these effects.

One can see that the metastable impurity states play an important role in a series of very unusual non-equilibrium effects observed in $Pb_{1-x}Sn_xTe(In)$. However, the main properties of these states, for example, the profile of the density of states, are not yet well established. There exist only some very vague estimations of what should be their main features. Substantial experimental and especially theoretical efforts are needed to clarify the situation.

9. Photodetector Systems Based on $Pb_{1-x}Sn_xTe(In)$: Applied Aspects

In this section we will consider the prospects of the application of the In-doped lead–tin tellurides in infrared photodetector systems. Some properties of these materials make the idea to use them as IR-photodetectors very attractive.

First of all, doping with In allows to obtain rather easily samples with very high spatial homogeneity of electric parameters and with very low background free carrier concentration, when the Fermi level is pinned within the gap.

Besides that, the lifetime of photoexcited electrons may be varied in a wide range (10^{-5} to 10^{5}) s by means of changing temperature or alloy composition. The parameters of $Pb_{1-x-y}Sn_xGe_yTe(In)$ photodetectors are $D^* = 1.7 \times 10^{13}$ cm $Hz^{1/2}$ W^{-1} at $T = 20$ K and $D^* = 10^{12}$ cm $Hz^{1/2}$ W^{-1} at $T = 40$ K [140].

Generally, integration of an incident radiation flux results in a considerable increase of the signal-to-noise ratio. However, for most photodetectors the output signal is proportional to the intensity of incident radiation, so external circuits or charge coupled devices are needed for the signal integration. This makes the technique of photodetector fabrication rather sophisticated, and the dynamical range of these devices is not very high. In case of $Pb_{1-x}Sn_xTe(In)$ this problem may be solved simply by lowering the temperature, and the photosignal is integrated due to the persistent photoconductivity effect. The microwave quenching of the persistent photoconductivity gives the possibility to restore quickly (within 1 to 10 μs) the initial state of the photodetector. This value gives the maximum operating rate of the photodetector ≈100 kHz to 1 MHz.

We have constructed a laboratory model of an IR-radiometer based on $Pb_{1-x}Sn_xTe(In)$ working in the regime of periodical accumulation and successive fast quenching of the persistent photoconductivity. Estimations of the detectivity of this radiometer gave $D^* \approx 10^{16}$ cm $Hz^{1/2}$ W^{-1} for the operating rate 100 Hz and the cut-off wavelength $\lambda \approx 50$ μm. The measurements were performed in the background-free regime.

The maximum operating rate is not very high. However, it may be not so important, for example, for the construction of a focal-plane matrix on $Pb_{1-x}Sn_xTe(In)$. Indeed, local illumination of the sample leads to local photogeneration, and excited electrons do not diffuse from the region of generation [167]. It means that the distribution of the radiation intensity on the sample surface is reflected in the distribution of long-living free electrons, so the sample itself is a kind of "continuous" matrix. Both contact and non-contact readout techniques are possible. However, these ideas are not yet realized in practice.

At last, the $Pb_{1-x}Sn_xTe(In)$ photodetectors are very stable with respect to the action of hard radiation. The measurements performed by Skipetrov and Ryabova [168] have shown that the photoresponse does not change after fast electron irradiation with fluences up to 10^{17} cm^{-2}. This value is at least by four orders of magnitude higher than for $Hg_{1-x}Cd_xTe$ or doped Ge and Si. This is the consequence of the Fermi level pinning effect.

The biggest disadvantage of $Pb_{1-x}Sn_xTe(In)$ photodetectors operating in the regime of internal integration is the very low operating temperature $T < 20$ K. Though the temperature must be lowered for any photodetector operating in the wavelength range $\lambda \approx 50$ μm, this restricts the field of possible applications of these photodetectors. In our opinion, the $Pb_{1-x}Sn_xTe(In)$-based photodetectors are ideal for infrared astronomy.

10. Concluding Remarks

The facts presented in the preceding sections have demonstrated a variety of non-equilibrium electron effects in MLTA. The experiments carried out in quantizing magnetic or high electric field, tunneling and optical data give unambiguous evidence for the existence of doping-induced quasi-localized electron levels in MLTA, and their main properties are found for some impurities. However, in other situations, for example, when infrared or microwave excitation is added, many unresolved questions remain. In addition, the information about the energy spectrum of the defects is insufficient and sometimes contradictory. It complicates the interpretation of the experimental data.

On the one hand, further investigations of the parameters of the doping-induced centres are necessary as the basis for a study of the non-equilibrium processes. The microscopic structure of the centres, the characteristics of their energy levels, and other parameters are to be established. Here different spectroscopic methods such as optical, tunneling, and maybe DLTS and acoustic spectroscopy could be very useful. The phase transitions in MLTA and their influence upon the electron properties also need further investigation.

On the other hand, the application of the powerful methods of the modern hot electron physics such as, e.g. time-resolved photoluminescence spectroscopy, spatially resolved absorption and luminescence measurements [169], the recently developed electron microscopy-based technique [170], spatially resolved photocurrent measurements [171] would give additional information on the carrier distributions in energy and space and on the relaxation processes. Then a better understanding of the complicated and interesting physics of the non-equilibrium electron phenomena in MLTA could be reached.

Acknowledgements

We are grateful to Prof. N. B. Brandt for his interest in these problems and helpful discussions. We thank Prof. V. P. Zlomanov for consultations in chemistry problems of material science and Prof. V. I. Kaidanov for helpful discussions. This work was supported in part by the program "Universities of Russia".

References

[1] B. I. SHKLOVSKII and A. L. EFROS, Electronic Properties of Doped Semiconductors, Springer-Verlag, New York 1984.
[2] Y. OOTUKA and A. KAWABATA, Progr. theor. Phys., Suppl. **84**, 249 (1985).
[3] H. PREIER, Appl. Phys. **20**, 189 (1989).
[4] G. H. DOEHLER, IEEE J. Quantum Electronics **22**, 1682 (1986).
[5] H. ZOGG, S. BLUNIER, T. HOSHINO, J. MASEK, and A. N. TIWARI, IEEE Trans. Electron Devices **5**, S49 (1991).
[6] J. B. CHOI, S. LIU, and H. D. DREW, Phys. Rev. B **43**, 4046 (1991).
[7] A. M. STONEHAM, Phil. Mag. **B51**, 161 (1985).
[8] V. I. KAIDANOV and S. A. NEMOV, Fiz. Tekh. Poluprov. **15**, 542 (1981) (Soviet Phys. – Semicond. **15**, 306 (1981)).
[9] V. I. KAIDANOV and YU. I. RAVICH, Uspekhi fiz. Nauk **145**, 51 (1985) (Soviet. Phys. – Usp. **28**, 31 (1985)).
[10] B. A. AKIMOV, N. B. BRANDT, B. S. KERNER, V. N. NIKIFOROV, and S. M. CHUDINOV, Solid State Commun. **43**, 31 (1982).
[11] B. A. AKIMOV, N. B. BRANDT, and V. N. NIKIFOROV, Fiz. tverd. Tela **26**, 1602 (1984) (Soviet Phys. – Solid State **26**, 973 (1984)).
[12] V. I. KAIDANOV, S. A. RYKOV, M. A. RYKOVA, and O. V. SYURIS, Fiz. Tekh. Poluprov. **24**, 144 (1990).
[13] B. A. AKIMOV, N. B. BRANDT, S. A. BOGOSLOVSKII, L. I. RYABOVA, and S. M. CHUDINOV, Zh. eksper. teor. Fiz., Pisma **29**, 11 (1979).
[14] A. V. NOVOSELOVA and V. P. ZLOMANOV, Current Topics in Material Science, Vol. 7, North-Holland Publ. Co., 1981 (p. 643).
[15] D. L. PARTIN, J. appl. Phys. **57**, 1997 (1985).
[16] B. A. AKIMOV, E. N. KOROBEYNIKOVA, L. I. RYABOVA, and M. E. TAMM, Fiz. Tekh. Poluprov. **25**, 342 (1991) (Soviet Phys. – Semicond. **25**, 208 (1991)).
[17] V. D. VULCHEV, L. D. BORISOVA, and S. K. DIMITROVA, phys. stat. sol. (a) **97**, K79 (1986).
[18] M. N. VINOGRADOVA, E. A. GURIEVA, V. I. JARSKII, S. V. ZARUBO, L. V. PROKOFIEVA, T. T. DEDEGKAEV, and I. I. KRYUKOV, Fiz. Tekh. Poluprov. **12**, 663 (1978) (Soviet Phys. – Semicond. **12**, 387 (1978)).

[19] B. A. AKIMOV, N. B. BRANDT, K. R. KURBANOV, L. I. RYABOVA, A. T. KHASANOV, and D. R. KHOKHLOV, Fiz. Tekh. Poluprov. **17**, 1604 (1983) (Soviet Phys. – Semicond. **17**, 1021 (1983)).
[20] L. M. KASHIRSKAYA, L. I. RYABOVA, O. I. TANANAEVA, and N. A. SHIROKOVA, Fiz. Tekh. Poluprov. **24**, 1349 (1990) (Soviet Phys. – Semicond. **24**, 848 (1990)).
[21] V. I. KAIDANOV, R. B. MELNIK, and I. A. CHERNIK, Fiz. Tekh. Poluprov. **7**, 759 (1973) (Soviet Phys – Semicond. **7**, 522 (1973)).
[22] S. N. LYKOV and I. A. CHERNIK, Fiz. Tekh. Poluprov. **14**, 47 (1980) (Soviet Phys. – Semicond. **14**, 25 (1980)).
[23] B. A. AKIMOV, P. V. VERTELETSKI, V. P. ZLOMANOV, L. I. RYABOVA, O. I. TANANAEVA, and N. A. SHIROKOVA, Fiz. Tekh. Poluprov. **23**, 244 (1989) (Soviet Phys. – Semicond. **23**, 151 (1989)).
[24] I. A. CHERNIK and S. N. LYKOV, Zh. Tekh. Fiz., Pisma **33**, 94 (1981) (Soviet Phys. – Tech. Phys., Letters **7**, 40 (1981)).
[25] V. I. KAIDANOV, S. A. NEMOV, R. V. PARFENEV, and D. V. SHAMSHUR, Zh. eksper. teor. Fiz., Pisma **35**, 517 (1982).
[26] A. V. NOVOSELOVA, V. P. ZLOMANOV, A. M. GASKOV, L. I. RYABOVA, M. A. LAZARENKO, and N. G. LISINA, Vestnik MGU, Ser. Khim. **23**, 3 (1982).
[27] K.-P. MOELLMANN, D. SICHE, and S. ZAJNUDINOV, Crystal Res. Technol. **21**, 1273 (1986).
[28] V. M. LAKEENKOV, V. V. TETERKIN, F. F. SIZOV, S. V. PLYATSKO, and S. A. BELOKON, Ukr. fiz. Zh. **29**, 757 (1984).
[29] G. S. BUSHMARINA, B. F. GRUZINOV, I. A. DRABKIN, E. YA. LEV, B. YA. MOIZHES, and S. G. SUPRUN, Izv. Akad. Nauk SSSR, Ser. neorg. Mater. **23**, 222 (1987) (Soviet Phys. – Inorg. Mater. **23**, 195 (1987)).
[30] A. N. VEIS, V. I. KAIDANOV, N. A. KOSTYLEVA, R. B. MELNIK, and YU. I. UKHANOV, Fiz. Tekh. Poluprov. **7**, 928 (1973) (Soviet Phys. – Semicond. **7**, 630 (1973)).
[31] B. A. AKIMOV, N. B. BRANDT, A. M. GASKOV, V. P. ZLOMANOV, L. I. RYABOVA, and D. R. KHOKHLOV, Fiz. Tekh. Poluprov. **17**, 87 (1983) (Soviet Phys. – Semicond. **17**, 53 (1983)).
[32] F. F. SIZOV, S. V. PLYATSKO, and V. M. LAKEENKOV, Fiz. Tekh. Poluprov. **19**, 592 (1985) (Soviet Phys. – Semicond. **19**, 368 (1985)).
[33] S. A. BELOKON, L. N. VERESHAGINA, I. I. IVANCHIK, L. I. RYABOVA, and D. R. KHOKHLOV, Fiz. Tekh. Poluprov. **26**, 264 (1992) (Soviet Phys. – Semicond. **26**, 148 (1992).
[34] L. I. BYTENSKII, V. I. KAIDANOV, V. P. MAKEENKO, R. B. MELNIK, and S. A. NEMOV, Fiz. Tekh. Poluprov. **18**, 489 (1984) (Soviet Phys. – Semicond. **18**, 303 (1984)).
[35] N. S. BESPALOVA, A. N. VEIS, and Z. M. DASHEVSKII, Fiz. Tekh. Poluprov. **21**, 946 (1987) (Soviet Phys. – Semicond. **21**, 577 (1987)).
[36] A. N. VEIS, Z. M. DASHEVSKII, and M. P. RULENKO, Fiz. Tekh. Poluprov. **24**, 128 (1990) (Soviet Phys. – Semicond. **24**, 76 (1990)).
[37] L. I. BYTENSKII, V. I. KAIDANOV, R. F. KUTEINIKOV, R. B. MELNIK, S. A. NEMOV, and YU. I. RAVICH, Fiz. Tekh. Poluprov. **15**, 981 (1981) (Soviet Phys. – Semicond. **15**, 563 (1981)).
[38] V. D. VULCHEV and L. D. BORISOVA, phys. stat. sol. (a) **99**, K53 (1987).
[39] B. A. AKIMOV, L. I. RYABOVA, S. M. CHUDINOV, and O. B. YATSENKO, Fiz. Tekh. Poluprov. **13**, 752 (1979) (Soviet Phys. – Semicond. **13**, 441 (1979)).
[40] S. TAKAOKA, T. ITOGA, and K. MURASE, Japan. J. appl. Phys. **23**, 216 (1984).
[41] B. A. AKIMOV, A. V. NIKORICH, L. I. RYABOVA, and N. A. SHIROKOVA, Fiz. Tekh. Poluprov. **23**, 1019 (1989).
[42] A. I. LEBEDEV and H. A. ABDULLIN, Fiz. Tekh. Poluprov. **18**, 624 (1984) (Soviet Phys. – Semicond. **18**, 388 (1984)).
[43] T. V. BOCHAROVA, A. N. VEIS, N. A. ERASOVA, and V. I. KAIDANOV, Fiz. Tekh. Poluprov. **16**, 1462 (1982) (Soviet Phys. – Semicond. **16**, 933 (1982)).
[44] B. A. AKIMOV, V. P. ZLOMANOV, L. I. RYABOVA, S. M. CHUDINOV, and O. B. YATSENKO, Fiz. Tekh. Poluprov. **13**, 1293 (1979) (Soviet Phys. – Semicond. **13**, 759 (1979)).
[45] B. A. AKIMOV, N. B. BRANDT, L. I. RYABOVA, D. R. KHOKHLOV, S. M. CHUDINOV, and O. B. YATSENKO, Zh. eksper. teor. Fiz., Pisma **31**, 304 (1980).
[46] B. A. AKIMOV, A. V. ALBUL, I. I. IVANCHIK, L. I. RYABOVA, E. I. SLYNKO, and D. R. KHOKHLOV, Fiz. Tekh. Poluprov. **27**, (1993), to be published.
[47] B. A. AKIMOV, S. A. BELOKON, Z. M. DASHEVSKII, K. N. EGOROV, V. M. LAKEENKOV, A. V. NIKORICH, and L. I. RYABOVA, Fiz. Tekh. Poluprov. **25**, 250 (1991).
[48] B. A. AKIMOV, N. B. BRANDT, L. I. RYABOVA, V. V. SOROVISHIN, and S. M. CHUDINOV, J. low-Temp. Phys. **51**, 9 (1983).

[49] B. A. AKIMOV, L. I. RYABOVA, and S. M. CHUDINOV, Fiz. tverd. Tela **21**, 708 (1979) (Soviet Phys. – Solid State **21**, 416 (1979)).
[50] S. TAKAOKA, T. ITOGA, and K. MURASE, Solid State Commun. **46**, 287 (1983).
[51] B. A. AKIMOV, N. B. BRANDT, L. I. RYABOVA, and V. V. SOKOVISHIN, Zh. eksper. teor. Fiz. **87**, 1349 (1984) (Soviet Phys. – J. exper. theor. Phys. **60**, 774 (1984)).
[52] B. M. VUL, I. D. VORONOVA, G. A. KALUZHNAYA, T. S. MAMEDOV, and T. SH. RAGIMOVA, Zh. eksper. teor. Fiz., Pisma **29**, 21 (1979).
[53] B. A. AKIMOV, N. B. BRANDT, S. O. KLIMONSKII, L. I. RYABOVA, and D. R. KHOKHLOV, Phys. Letters A **88**, 483 (1982).
[54] B. A. AKIMOV, V. P. ZLOMANOV, L. I. RYABOVA, and D. R. KHOKHLOV, Vysokochistye veshestva **6**, 22 (1991).
[55] B. A. VOLKOV, I. D. VORONOVA, and A. P. SHOTOV, Dokl. Akad. Nauk SSSR **293**, 602 (1987) (Soviet Phys. – Doklady **32**, 226 (1987).
[56] B. M. VUL, I. D. VORONOVA, S. P. GRISHECHKINA, and T. SH. RAGIMOVA, Zh. eksper. teor. Fiz., Pisma **33**, 346 (1981).
[57] A. MARTINEZ, R. J. ABBUNDI, J. L. DAVIS, B. B. HOUSTON, and R. S. ALLGAIER, J. appl. Phys. **57**, 1165 (1985).
[58] A. MARTINEZ, F. SANTIAGO, J. L. DAVIS, and B. HOUSTON, J. appl. Phys. **58**, 4618 (1985).
[59] K.-P. MOELLMANN, K. H. HERRMANN, and R. ENDERLEIN, Proc. 16th Internat. Conf. Phys. Semicond., Montpellier 1982; Physica (Utrecht) **117/118B**, 582 (1983).
[60] K. H. HERRMANN, K.-P. MÖLLMANN, and M. WENDT, phys. stat. sol. (a) **80**, 541 (1983).
[61] A. I. LEBEDEV and T. D. AITIKEEVA, Fiz. Tekh. Poluprov. **18**, 1964 (1984) (Soviet Phys. – Semicond. **18**, 1227 (1984)).
[62] YU, G. TROYAN, F. F. SIZOV, and V. M. LAKEENKOV, Fiz. Tekh. Poluprov. **20**, 1776 (1986) (Soviet Phys. – Semicond. **20**, 1113 (1986)).
[63] B. A. AKIMOV, N. B. BRANDT, A. V. NIKORICH, L. I. RYABOVA, and V. V. SOKOVISHIN, Zh. eksper. teor. Fiz., Pisma **39**, 222 (1984) (Soviet Phys. – J. exper. theor. Phys., Letters **39**, 265 (1984)).
[64] I. I. ZASAVITSKII, A. V. MATVEENKO, B. N. MATSONASHVILI, and V. T. TROFIMOV, Fiz. Tekh. Poluprov. **21**, 1789 (1987) (Soviet Phys. – Semicond. **21**, 1084 (1987)).
[65] I. I. ZASAVITSKII, B. N. MATSONASHVILI, and V. T. TROFIMOV, Fiz. Tekh. Poluprov. **23**, 2019 (1989) (Soviet Phys. – Semicond. **23**, 1249 (1989)).
[66] K. SEEGER, Semiconductor Physics, Chap. 12, § 2, Springer-Verlag, Wien/New York 1973.
[67] A. M. STONEHAM, Theory of Defects in Solids, Oxford University Press, 1975.
[68] R. W. GURNEY and N. F. MOTT, Trans. Faraday Soc. **35**, 69 (1939).
[69] D. V. LANG and R. A. LOGAN, Phys. Rev. Letters **39**, 635 (1977).
[70] YU. M. KAGAN and K. A. KIKOIN, Zh. eksper. teor. Fiz. Pisma **31**, 367 (1980).
[71] I. A. DRABKIN and B. YA. MOIZHES, Fiz. Tekh. Poluprov. **17**, 969 (1983) (Soviet Phys. – Semicond. **17**, 611 (1983)).
[72] V. I. LITVINOV and K. D. TOVSTYUK, Fiz. tverd. Tela **24**, 896 (1982) (Soviet Phys. – Solid State **24**, 508 (1982)).
[73] B. A. VOLKOV and O. A. PANKRATOV, Dokl. Akad. Nauk SSSR **255**, 93 (1980) (Soviet Phys. – Doklady **25**, 922 (1980)); Zh. eksper. teor. Fiz. **88**, 280 (1985) (Soviet Phys. – J. exper. theor. Phys. **61**, 164 (1985)).
[74] O. A. PANKRATOV and B. A VOLKOV, Soviet Sci. Rev. A (Physics) **9**, 355 (1987).
[75] O. A. PANKRATOV and P. P. POVAROV, Solid State Commun. **66**, 847 (1988).
[76] P. W. ANDERSON, Phys. Rev. Letters **34**, 953 (1985).
[77] G. NIMTZ and B. SCHLICHT, Narrow Gap Lead Salts, in: Narrow-Gap Semiconductors, Ed. G. HÖHLER, Springer-Verlag, Berlin 1983.
[78] L. D. LANDAU and E. M. LIFSHITZ, Quantum Mechanics: Non-Relativistic Theory, 3rd ed., Pergamon Press, Oxford 1977.
[79] M. L. GOLDBERGER and K. M. WATSON, Collision Theory, Wiley, New York 1964.
[80] O. F. SANKEY, J. D. DOW, and K. HESS, Appl. Phys. Letters **41**, 664 (1982).
[81] V. V. BONDARENKO, V. A. SHENDEROVSKII, and V. V. TETYORKIN, Ukr. fiz. Zh. **36**, 440 (1991).
[82] D. CHATTOPADHYAY, H. AICHMANN, and G. NIMTZ, Solid State Commun. **51**, 151 (1984).
[83] A. KROTKUS and Z. DOBROVOLSKIS, Electrical Conductivity of Narrow-Gap Semiconductors, Mokslas, Vilnius 1988 (in Russian).

[84] K. R. KURBANOV, A. M. PALKIN, E. V. SKUBNEVSKII, and E. T. STANKEVICH, Fiz. Tekh. Poluprov. **22**, 1509 (1988).
[85] D. CHATTOPADHYAY and N. N. PURKAIT, J. appl. Phys. **54**, 6439 (1983).
[86] P. N. GORLEY and V. A. SHENDEROVSKII, Transport Phenomena in Narrow Gap Semiconductors PbTe, $Pb_{1-x}Sn_xTe$, PbSe, Preprint Inst. Phys. Ukr. Acad. Sci., Kiev 1979 (in Russian).
[87] P. M. TOMCHUK, V. A. SHENDEROVSKII, P. N. GORLEY, and N. P. GAVALESHKO, phys. stat. sol. (b) **118**, 433 (1983).
[88] E. M. CONWELL, High Field Transport in Semiconductors, Academic Press, New York/London 1967.
[89] F. G. BASS and YA. G. GUREVICH, Hot Electrons and Strong Electromagnetic Waves in the Plasmas of Semiconductors and Gas Discharge, Izd. Nauka, Moscow 1975 (in Russian).
[90] V. L. BONCH-BRUEVICH and S. G. KALASHNIKOV, Physics of Semiconductors, 2nd ed., Izd. Nauka, Moscow 1991.
[91] YU. I. RAVICH, B. A. EFIMOVA, and V. I. TAMARCHENKO, phys. stat. sol. (b) **43**, 453 (1971).
[92] A. KROTKUS, T. LIDEIKIS, P. PLITNIKAS, and I. SIMKIENE, Solid State Electronics **26**, 605 (1983).
[93] V. F. GANTMAKHER and I. B. LEVINSON, Scattering of Current Carriers in Metals and Semiconductors, North-Holland Publ. Co., Amsterdam 1987.
[94] B. PÖDÖR, phys. stat. sol. (b) **134**, K145 (1986).
[95] L. PALMETSCHOFER, K. H. GRESSLEHNER, L. RATCHBACHER, and A. LOPEZ-OTERO, Lecture Notes Phys. **152**, 391 (1982).
[96] H. ST-ONGE and I. N. WALPOLE, Phys. Rev. B **6**, 2337 (1972).
[97] J. JANTSCH, J. ROZENBERGS, and H. HEINRICH, Solid State Electronics **21**, 103 (1972).
[98] S. D. BENESLAVSKII and A. V. DMITRIEV, Fiz. tverd. Tela **20**, 1668 (1978) (Soviet, Phys. – Solid State **20**, 966 (1978)).
[99] S. D. BENESLAVSKII and A. V. DMITRIEV, Solid State Commun. **32**, 1175 (1979).
[100] A. N. ZAITSEV and A. K. ZVEZDIN, Zh. eksper. teor. Fiz., Pisma **10**, 8 (1969).
[101] S. D. BENESLAVSKII, A. V. DMITRIEV, and N. S. SALIMOV, Zh. eksper. teor. Fiz. **92**, 305 (1987) (Soviet Phys. – J. exper. theor. Phys. **65**, 173 (1987)).
[102] A. V. DMITRIEV, Solid State Commun. **74**, 2137 (1990).
[103] A. I. BAZ, Yadernaya Fiz. **5**, 229 (1967) (Soviet Phys. – J. nuclear Phys. **5**, 161 (1967)).
[104] E. M. LIFSHITS and L. P. PITAEVSKII, Physical Kinetics, Izd. Nauka, Moscow 1979.
J. H. FERZIGER and H. G. KAPER, Mathematical Theory of Transport Processes in Gases, North-Holland Publ. Co., Amsterdam/London 1972.
[105] V. L. BONCH-BRUEVICH, I. P. ZVYAGIN, and A. G.MIRONOV, Domain Electrical Instabilities in Semiconductors, Consultants Bureau, New York/London 1975.
[106] S. D. BENESLAVSKII and N. S. SALIMOV, Izv. vuzov, Fizika **32**, 74 (1989).
[107] V. I. KAIDANOV, S. A. RYKOV, and M. A. RYKOVA, Fiz. tverd. Tela **31**, 68 (1989).
[108] B. RICCO and M. AZBEL, Phys. Rev. B **29**, 1970 (1984).
[109] A. KROTKUS, P. PLITNIKAS, and I. SIMKIENE, Fiz. Tekh. Poluprov. **17**, 2180 (1983) (Soviet Phys. – Semicond. **17**, 1393 (1983)).
[110] W. JANTSCH, J. ROZENBERGS, and H. HEINRICH, Solid State Commun. **17**, 1145 (1975).
[111] A. KROTKUS, T. LIDEIKIS, A. PLITNIKAS, and S. ZHURAUSKAS, Litovski Fiz. Sbornik **26**, 582 (1986).
[112] H. ST-ONGE, F. G. LEONBERGER, and J. N. WALPOLE, J. Nonmetals **2**, 49 (1973).
[113] B. A. AKIMOV, D. R. KHOKHLOV, and S. N. CHESNOKOV, Fiz. Tekh. Poluprov. **23**, 899 (1989).
[114] YU. A. ABRAMYAN, K. Z. PAPAZYAN, and V. I. STAFEEV, Fiz. Tekh. Poluprov. **24**, 1752 (1990).
[115] B. A. AKIMOV, N. B. BRANDT, K. N. EGOROV, R. V. LUTSIV, S. N. CHESNOKOV, and D. R. KHOKHLOV, Fiz. Tekh. Poluprov. **21**, 1379 (1987) (Soviet Phys. – Semicond. **21**, 839 (1987)).
[116] B. A. AKIMOV, A. V. ALBUL, E. V. BOGDANOV, and V. YU. ILYIN, Fiz. Tekh. Poluprov. **26**, 1300 (1992).
[117] N. F. MOTT and E. A. DAVIS, Electron Processes in Non-Crystalline Materials, 2nd ed., Clarendon Press, Oxford 1979.
[118] B. I. SHKLOVSKII, Fiz. Tekh. Poluprov. **10**, 1440 (1976) (Soviet Phys. – Semicond. **10**, 855 (1976)).
[119] K. MURASE and S. NISHI, Lecture Notes Phys. **152**, 261 (1982).
[120] R. TRIBULET, G. DIDIER, and A. LASHBLEY, Lecture Notes Phys. **152**, 54 (1982).
[121] M. HAPP and K.-P. MÖLLMANN, phys. stat. sol. (a) **91**, K159 (1985).
[122] K. H. HERRMANN, G. A. KALYUZHNAYA, K.-P. MÖLLMANN, and M. WENDT, phys. stat. sol. (a) **71**, K21 (1982).

[123] K. H. HERRMANN and K.-P. MÖLLMANN, phys. stat. sol. (a) **80**, K101 (1983).
[124] V. N. VINCHAKOV, V. I. KAIDANOV, S. N. LYKOV, and S. A. RYKOV, Zh. eksper. teor. Fiz., Pisma **43**, 384 (1986) (Soviet Phys. – J. exper. theor. Phys., Letters **43**, 495 (1986)).
[125] V. N. VINCHAKOV, V. I. KAIDANOV, and S. A. RYKOV, Fiz. Tekh. Poluprov. **15**, 2235 (1981) (Soviet Phys. – Semicond. **15**, 1296 (1981)).
[126] A. N. VEIS and R. R. YAFAEV, Fiz. Tekh. Poluprov **18**, 475 (1984) (Soviet Phys. – Semicond. **18**, 295 (1984)).
[127] A. N. VEIS and E. V. GLEBOVA, Izv. vuzov, Fizika **26**, 117 (1983).
[128] I. A. DRABKIN, B. A. EFIMOVA, G. F. ZAKHARUGINA, V. I. KAYDANOV, R. B. MELNIK, and I. V. NELSON, Fiz. Tekh. Poluprov. **7**, 794 (1973) (Soviet Phys. – Semicond. **7**, 545 (1973)).
[129] A. N. VEIS, V. I. KAIDANOV, and S. A. NEMOV, Fiz. Tekh. Poluprov. **12**, 1599 (1978) (Soviet Phys. – Semicond. **12**, 943 (1978)).
[130] T. V. BOCHAROVA, A. N. VEIS, Z. M. DASHEVSKII, V. A. KOTELNIKOV, and R. YU. KRUPITSKAYA, Fiz. Tekh. Poluprov. **15**, 175 (1981) (Soviet Phys. – Semicond. **15**, 103 (1981)).
[131] A. N. VEIS, V. I. KAYDANOV, YU. I. RAVICH, I. A. RYABTSEVA, and YU. I. UKHANOV, Fiz. Tekh. Poluprov. **10**, 104 (1976) (Soviet Phys. – Semicond. **10**, 62 (1976)).
[132] T. LIDEIKIS, A. PETRAITIENE, N. SIKTOROV, and I. SIMKIENE, Solid State Commun. **57**, 583 (1986).
[133] S. TAKAOKA and K. MURASE, J. Phys. Soc. Japan **52**, 25 (1983).
[134] B. A. AKIMOV, N. B. BRANDT, L. I. RYABOVA, and D. R. KHOKHLOV, Zh. tekh. Fiz., Pisma **6**, 1269 (1980) (Soviet Phys. – J. tech. Phys., Letters **6**, 544 (1980)).
[135] H. A. ABDULLIN and A. I. LEBEDEV, Fiz. Tekh. Poluprov. **19**, 1725 (1985) (Soviet Phys. – Semicond. **19**, 1061 (1985)).
[136] H. A. ABDULLIN and A. I. LEBEDEV, Zh. eksper. teor. Fiz., Pisma **39**, 272 (1984) (Soviet Phys. – J. exper. theor. Phys., Letters **39**, 325 (1984)).
[137] K. H. HERRMANN and K.-P. MÖLLMANN, phys. stat. sol. (a) **91**, K147 (1985).
[138] K.-P. MÖLLMANN and M. HAPP, phys. stat. sol. (a) **91**, K71 (1985).
[139] S. W. MCKNIGHT and M. K. EL-RAYESS, Semicond. Sci. Technol. **6**, C42 (1991).
[140] V. F. CHISHKO, V. T. HRYAPOV, I. L. KASATKIN, V. V. OSIPOV, E. I. SLINKO, O. V. SMOLIN, and V. V. TRETINIK, Infrared Phys. **33**, 197 (1992).
[141] I. I. ZASAVITSKII, B. N. MATSONASHVILI, O. A. PANKRATOV, and V. T. TROFIMOV, Zh. eksper. teor. Fiz., Pisma **42**, 3 (1985) (Soviet Phys. – J. exper. theor. Phys., Letters **42**, 1 (1985)).
[142] I. I. ZASAVITSKII, A. V. MATVEENKO, B. N. MATSONASHVILI, and V. T. TROFIMOV, Fiz. Tekh. Poluprov. **20**, 214 (1986) (Soviet Phys. – Semicond. **20**, 135 (1986)).
[143] K.-P. MÖLLMANN, phys. stat. sol. (b) **149**, 663 (1988).
[144] A. I. BELOGOROKHOV, E. I. SLYNKO, and D. R. KHOKHLOV, Zh. Tekh. Fiz., Pisma **18**, 30 (1992).
[145] F. F. SIZOV, YU. G. TROYAN, and L. F. LINNIK, Ukr. fiz. Zh. **30**, 1225 (1985).
[146] K. H. HERRMANN, K.-P. MÖLLMANN, and M. WENDT, phys. stat. sol. (a) **80**, 541 (1983).
[147] A. V. DMITRIEV, Fiz. tverd. Tela **32**, 3647 (1990).
[148] YU. G. TROYAN, F. F. SIZOV, and V. M. LAKEENKOV, Ukr. fiz. Zh. **32**, 467 (1987).
[149] K. TAKASAKI and S. TANAKA, phys. stat. sol. (a) **40**, 173 (1977).
[150] S. W. MCKNIGHT and M. K. EL-RAYESS, Solid State Commun. **49**, 1001 (1984).
[151] S. W. MCKNIGHT and M. K. EL-RAYESS, J. Phys. C **17**, 6893 (1984).
[152] S. TAKAOKA, T. HAMAGUSHI, S. SHIMOMURA, and K. MURASE, Solid State Commun. **54**, 99 (1985).
[153] T. ISHIGUSHI and H. W. DREW, 17-th ICPS, San Fransisco (Ca) 1984, Book of Abstracts (p. 319).
[154] N. ROMCEVIC, Z. V. POPOVIC, D. KHOKHLOV, A. V. NIKORICH, and W. KONIG, Phys. Rev. B **43**, 6712 (1991).
[155] B. A. AKIMOV, A. V. NIKORICH, D. R. KHOKHLOV, and S. N. CHESNOKOV, Fiz. Tekh. Poluprov. **23**, 668 (1989) (Soviet Phys. – Semicond. **23**, 418 (1989)).
[156] A. I. BELOGOROKHOV, S. A. BELOKON, I. I. IVANCHIK, and D. R. KHOKHLOV, Fiz. tverd. Tela **34**, 1651 (1992).
[157] YU. A. PUSEP and M. P. SINUKOV, Zh. eksper. teor. Fiz., Pisma **45**, 449 (1987) (Soviet Phys. – J. exper. theor. Phys., Letters **45**, 575 (1987)).
[158] D. R. KHOKHLOV, A. DE VISSER, I. I. IVANCHIK, and A. V. NIKORICH, Physica (Utrecht) **177B**, 491 (1992).
[159] A. DE VISSER, I. I. IVANCHIK, A. V. NIKORICH, and D. R. KHOKHLOV, Fiz. Tekh. Poluprov. **26**, 1034 (1992).

[160] D. R. KHOKHLOV, I. I. IVANCHIK, A. DE VISSER, and A. V. NIKORICH, Solid State Commun. **82**, 759 (1992).
[161] I. I. IVANCHIK, A. V. NIKORICH, Z. POPOVICH, N. ROMCHEVICH, and D. R. KHOKHLOV, Proc. VIII. All-Union Symp. Narrow-Gap Semicond., Part II, Lvov 1991 (p. 107) (in Russian).
[162] B. A. AKIMOV, N. B. BRANDT, D. R. KHOKHLOV, and S. N. CHESNOKOV, Zh. Tekh. Fiz., Pisma **14**, 731 (1988) (Soviet Phys. – J. tech. Phys., Letters **14**, 325 (1988)).
[163] K. H. HERRMANN and K.-P. MÖLLMANN, phys. stat. sol. (b) **76**, K67 (1983).
[164] K. P. MÖLLMANN and M. HAPP, phys. stat. sol. (b) **134**, K75 (1986).
[165] B. A. AKIMOV, N. B. BRANDT, S. N. CHESNOKOV, and D. R. KHOKHLOV, Mater. Res. Soc. Symp. Proc. **216**, 147 (1991).
[166] D. E. DOLZHENKO, I. I. IVANCHIK, A. V. NIKORICH, D. R. KHOKHLOV, and S. N. CHESNOKOV, Zh. eksper. teor. Fiz., Pisma **55**, 125 (1992) (Soviet Phys. – J. exper. theor. Phys., Letters **55**, 119 (1992)).
[167] B. A. AKIMOV, N. B. BRANDT, S. N. CHESNOKOV, K. N. EGOROV, and D. R. KHOKHLOV, Solid State Commun. **66**, 811 (1988).
[168] E. P. SKIPETROV and L. I. RYABOVA, unpublished.
[169] R. SYMANCZYK, E. PIEPER, and D. JAEGER, Phys. Letters A **143**, 337 (1990).
[170] A. BRANDL, M. VOELCKER, and W. PRETTL, Solid State Commun. **72**, 847 (1989).
[171] K. M. MAYER, J. PARISI, U. RAU, J. PEINKE, and R. H. HUEBENER, Solid State Commun. **73**, 369 (1990).
[172] I. V. KUCHERENKO, L. M. KASHIRSKAYA, K.-P. MÖLLMANN, and E. S. ITSKEVICH, Fiz. Tekh. Poluprov. **23**, 1784 (1989).

(Received January 22, 1993)